# THE EFFECT OF AIR IN DAMPING WATER BORNE PRESSURE PULSES

WILLIAM A. REHDER

# THE EFFECT OF AIR IN DAMPING WATER BORNE PRESSURE PULSES

* * * * *

William A. Rehder

# THE EFFECT OF AIR IN

# DAMPING WATER BORNE PRESSURE PULSES

by

William A. Rehder

Lieutenant, United States Navy

Submitted in partial fulfillment of
the requirements for the degree of

MASTER OF SCIENCE
IN
MECHANICAL ENGINEERING

United States Naval Postgraduate School
Monterey, California

1 9 6 4

# THE EFFECT OF AIR IN DAMPING WATER BORNE PRESSURE PULSES

by

William A. Rehder

This work is accepted as fulfilling
the thesis requirements for the degree of
MASTER OF SCIENCE
IN
MECHANICAL ENGINEERING
from the
United States Naval Postgraduate School

ABSTRACT

The effect of injection of up to ten percent by volume air in damping the amplitude of water borne pressure pulses was studied. Pressure pulses were generated using a water hammer model. The water hammer model consisted of a length of pipe with water flowing through it and a quick closing valve located downstream. Measured amounts of air were injected into a water stream and the valve was quickly closed. The pressure-time history was recorded on oscilloscope photographs at two locations along the pipe. A mathematical model was developed for this two phase model. Small amounts of air greatly reduced the amplitude of the pressure pulses. By injection of one percent by volume of air into the model at 15.5 psia, the pressure amplitude was reduced to 8.6 percent of the theoretical no air amplitude. The effect decreased with increased pressure of the system.

ACKNOWLEDGMENTS

The writer wishes to express his appreciation to Professor Paul F. Pucci for his assistance and encouragement during this project. He also wishes to thank Mr. Kenneth Mcthersell for his welding and machine work. A special thank you goes to Mr. Joseph Beck for his assistance in construction, assembly and instrumentation of the project. For the rough typing, the writer wishes to express appreciation to his wife, Vina.

TABLE OF CONTENTS

LIST OF ILLUSTRATIONS

TABLE OF SYMBOLS AND ABBREVIATIONS

| Symbol | Meaning | Units |
|---|---|---|
| A | Inside cross sectional area of pipe | $ft^2$ |
| C | psi/cm of oscilloscope deflection | psi/cm |
| D | Pipe diameter | ft or in |
| E | Modulus of elasticity of pipe | $lbf/ft^2$ |
| F | Force | lbf |
| G | Volume | $ft^3$ |
| H | Head of water | ft of water |
| $H_y$ | Head rise above the initial static no flow static head | ft of water |
| J | Correction of measured pressure for velocity head | psi |
| K | Bulk modulus of water | $lbf/ft^2$ |
| L | Length of pipe (from valve to tank) | ft |
| M | Mass | slugs |
| P | Pressure | psi |
| Q | Volume flow rate | $ft^3/min$ |
| R | Gas constant (53.3 for air) | ft-lbf/lbm°F |
| S | Stress in pipe | psi |
| T | Absolute temperature | °R |
| V | Velocity | ft/min or ft/sec |
| X | Distance to any position on the pipe measured from the valve | ft |
| a | Velocity of pressure pulse in the fluid | ft/sec |
| c | Barometer temperature correction | in. Hg |
| d | Deflection on oscilloscope photograph | cm |

Table of Symbols and Abbreviations (Cont'd)

| Symbol | Meaning | Units |
|---|---|---|
| e | Pipe wall thickness | ft. or in. |
| $g_o$ | Proportionality constant in Newton's 2nd law of motion ($F = \frac{1}{g_o} M\ddot{x}$) | $\frac{lbm}{lbf} \frac{ft}{sec^2}$ |
| g | Acceleration of gravity | $ft/sec^2$ |
| k | Ratio of specific heats at constant pressure to that at constant volume. 1.403 for air. | |
| $\dot{m}$ | Mass flow rate | lbm/min |
| m | Mass | lbm |
| s | Distance | ft or in |
| t | Temperature | °F |
| $t_i$ | Time | sec or min |
| x | Volume fraction air in water | |
| $\rho$ | Density | $slugs/ft^3$ |
| $\eta$ | Volume percent air at water inlet conditions of temperature and pressure | % |
| $\eta_{WT}$ | Weight percent air | % |
| | Compressibility 1/K | $ft^2/lbf$ |
| $\tau$ | Period of pressure wave | sec |
| $\gamma$ | Specific weight | $lbf/ft^3$ |

SUBSCRIPTS

| | |
|---|---|
| A | Adiabatic |
| a | Air |
| c | Combined air and water mixture |
| e | Outside |
| i | Inside |
| I | Isothermal |

Subscripts (Cont'd)

| Symbol | Meaning |
|---|---|
| m | Maximum |
| n or N | No air |
| o | Initial conditions |
| p | Pipe |
| T | Theoretical |
| u | Uncorrected |
| w | Water |
| Ia | Isothermal air |
| Aa | Adiabatic air |
| aw | Air at conditions of water inlet |
| NT | No air, theoretical |
| ATM | Atmospheric conditions |
| ABS | Absolute |

## 1. Introduction.

In recent years the United States Navy has been doing a great deal of research and development in methods of reducing the noise level of machinery for submarines and for anti-submarine ships. The fluid systems of these ships transmit noises via pressure pulses in the systems' contents. A similar problem concerning fluid borne pressure pulses is that of vibrations set up by water hammer in piping systems. The objective of this study was to quantitatively determine the effect of air in damping water borne pressure pulses.

## 2. Theory.

To study the effect of air in damping water borne pressure pulses, it was necessary to generate a pressure pulse in the liquid. For this study, the water hammer model was used to generate the pressure pulse. The water hammer model shown in Fig. 1 consists essentially of a head tank, a length of pipe, and a quick closing valve. The water is allowed to flow through the pipe with a velocity head. If the valve is quickly closed, this velocity head is immediately changed to pressure head which in turn sends a pressure pulse down the pipe. This pressure wave travels down the pipe at the speed of sound in the fluid contained in the system.

Considering the system shown in Fig. 1, the maximum pressure rise by instantaneously closing the valve is given by the following equation.

$$H_y = \frac{V_o a}{g_o} \tag{1}$$

Where: $H_y$ = Head rise above the initial static no flow head, ft. of water

$V_o$ = Velocity of the water in the pipe before valve closure, ft/sec.

$g_o$ = Proportionality constant in Newton's second law of motion, $(lbm\text{-}ft)/(lbf\text{-}sec^2)$.

$a$ = Velocity of the pressure pulse, ft/sec.

The derivation of this equation as derived by Stepanoff /13/ is included in Appendix B. This equation does not include frictional effects. If the valve is closed instantaneously, the maximum pressure given by equation (1) will be the same along the whole length of the pipe. Obviously, a valve cannot be closed instantaneously. However, this same maximum pressure rise at a given location A along the pipe will be attained if the valve is closed in less time than it takes the pressure pulse to travel from position A to the tank and to reflect back to position A. At the

valve, the time for the pressure pulse to reflect back is $2L/a$. Where L is the length of the pipe from the valve to the tank. At the center of the pipe, the time for the pressure pulse to reflect back is $L/a$. Next to the tank the maximum pressure will not be attained unless the valve is closed instantaneously. For the maximum pressure given by equation (1) to be attained at a given point located at a distance X from the valve, the closure time must be less than $2(L-X)/a$.

The speed of the pressure wave in a pure water pipe system is given by

$$a = \frac{1}{\sqrt{\rho_w \left( 1/K_w + \frac{D}{eE} \right)}} \qquad (2)$$

Where: $\rho_w$ = Water density, slugs/ft$^3$

$K_w$ = Water bulk modulus, lbf/ft$^2$.

D = Inside pipe diameter, in.

e = Pipe wall thickness, in.

E = Pipe modulus of elasticity.

This equation has been derived in Appendix B. This equation can be extended to a two phase air-water system. The speed of a pressure pulse based upon an isothermal compression of the air by the pressure pulse is given by

$$a_I^{-2} = \frac{x k}{a_a^2} + \frac{(1-x)^2}{a_w^2} + x(1-x)\left[ \frac{\rho_w}{P_{ABS}} + \rho_a \mathcal{K}_w \right] + \frac{D}{eE}\left[ (1-x)\rho_w + x\rho_a \right] \qquad (3)$$

Where: x = Volume fraction air at water inlet conditions.

$a_I$ = Velocity of the pressure pulse in the air-water mixture with isothermal compression of the air by the pressure pulse, ft/sec.

$a_a$ = Velocity of sound in air at the temperature of the fluid, ft/sec.

$a_w$ = Velocity of sound in water at the temperature of the fluid, ft/sec.

k = Ratio of specific heats at constant pressure to that at constant volume for air.

$P_{ABS}$ = Absolute pressure of the system, $lbf/ft^2$.

$\rho_a$ = Air density, $slugs/ft^3$

$\mathcal{K}_w$ = Compressibility of water, $ft^2/lbf$.

The speed of the pressure pulse based upon an adiabatic compression of the air by the pressure pulse is given by:

$$a_A^{-2} = \frac{x}{a_a^2} + \frac{(1-x)^2}{a_w^2} + x(1-x)\left[\frac{\rho_w}{P_{ABS}\, k} + \rho_a \mathcal{K}_w\right] + \frac{D}{eE}\left[(1-x)\rho_w + x\rho_a\right] \qquad (3a)$$

Equations (3) and (3a) have been derived in Appendix B. It is noted that equations (3) and (3a) reduce to equation (2) when no air is present. Substituting equation (2) into equation (1) and multiplying by the specific weight of water ($\gamma_w$), gives the maximum pressure rise upon valve closure with no air in the pipe.

$$H_y \gamma_w = P_{NT} = \frac{V_o \gamma_w}{g_o \sqrt{\rho_w \left(\frac{1}{K_w} + \frac{D}{eE}\right)}} \qquad (4)$$

The maximum pressure rise for an air-water mixture based upon isothermal compression of air is given by:

$$P = \frac{V_o \gamma_c a_I}{g_o} \qquad (5)$$

The term $a_I$ is given by equation (3). The derivation of equation (5) is in Appendix B. The same equation based upon adiabatic compression of the

air is given by:

$$P = \frac{V_o \gamma_c a_A}{g_o} \tag{5a}$$

The term $a_A$ is given by equation (3a). The derivation of equation (5a) is in Appendix B. The ratio of equation (5) to equation (4) gives:

$$\left(\frac{P}{P_{NT}}\right)_T = \frac{\gamma_c a_I}{\gamma_w} \sqrt{\rho_w \left(\frac{1}{K_w} + \frac{D}{eE}\right)} \tag{6}$$

The ratio of equation (5a) to equation (4) gives:

$$\left(\frac{P}{P_{NT}}\right)_T = \frac{\gamma_c a_A}{\gamma_w} \sqrt{\rho_w \left(\frac{1}{K_w} + \frac{D}{eE}\right)} \tag{6a}$$

If equation (6a) is used, adiabatic conditions are assumed or if equation (6) is used, isothermal conditions are assumed. Normally, sound traveling in the atmosphere is adiabatic. Karplus /4/ conducted experiments with air bubbles approximately 0.01 centimeters in diameter in an air-water mixture and found that his experimental data was best correlated by assuming an isothermal compression. The method used to inject air for this investigation did not give the small bubble distribution Karplus obtained. In Karplus' method, there was a high heat transfer surface per unit bubble volume. Therefore, the compression was nearly isothermal in the water. With larger bubbles there is less surface per unit bubble volume and the situation is probably best described by the adiabatic equation (6a).

Equation (6a) provides the fundamental theory for the damping of pressure pulses in water by air injection. By measuring the air injection rate, the water flow rate, and the pressure-time history at a given location in the system of Fig. 1, the effect of air in damping a pressure pulse in water is obtained. In this report, the experimental pressures obtained are compared with the theoretical relationship of equation (6a).

3. Equipment.

To study the effect of air in damping water borne pressure pulses, and to verify the applicability of equation (6a) to the water hammer model, the system shown in Fig. 1 was constructed.

The system consisted of 1) a head tank, a pipe and a weigh tank system 2) an air injection system 3) a valve and closure system and 4) a pressure recording system. A general description for each part of the system will be presented here. Exact detailed equipment specifications are included in Appendix C.

The head tank was a tank two feet in diameter with four constant head overflow sections. These overflow sections were located nominally at two, four, six and eight feet above the main tank outlet line. The main pipe length consisted of 59 feet 6 and 7/8 inches of two inch extra strong black steel pipe. This pipe was supported at ten feet intervals by a timber structure. At the main pipe discharge, a 20 inch by 28 inch by 20 inch weigh tank, platform scale and electric timer were used to measure the weight flow rate of the water. Water for the system was supplied from the city water supply.

The air injection system contained a Fischer and Porter Company rotometer with a glass ball float for air flow measurement. This rotometer had a maximum capacity of 0.325 cubic feet per minute at 14.7 psia and 70°F. Compressed air from a nominal 100 psig compressor was reduced by a regulating valve to approximately fifteen psig. A mercury manometer was used to measure the air pressure, and the air temperature was measured with a copper constantan thermocouple junction upstream of the rotometer. The air was transferred from the regulating valve to the point of injection through one quarter inch vinyl tubing. The air was regulated by a manual

control valve located immediately following the rotometer. Fig. 1 shows a diagram of the system. Fig. 2 shows a photograph of the component parts of the air injection system. The air was injected into the pipe near the tank through a system of three circles of small holes drilled equally spaced around the circumference of the pipe. Details are included in Appendix C. A concentric plexiglass cylinder with "O" ring seals surrounds these holes. The system was designed so that any one, any two, or any three of the circles of holes could be used to inject air at any one time. Fig. 5 shows a cross sectional view of the air inject annular ring. This method for air injection is very simple and could easily be adapted in practical applications.

If the same maximum pressure (neglecting friction losses) was to be obtained along one half the length of the pipe, it was necessary to close the valve in less than one half the pipe period $\left(\frac{L}{a}\right)$. This was obtained by the use of a modified two-inch Crane quick-closing valve. A steel cylinder two inches in diameter and one inch high was screwed onto the top of the stem. The valve was closed by dropping a seven pound weight from nine feet onto the cylinder. A spring loaded catch was provided to keep the valve closed when the valve was in the shut position. An isolated stop stand was provided for stopping the valve. This stop stand minimized the effect of the valve stopping impact from being transmitted to the pipe and to the valve body. A quick release mechanism was provided to release the weight which was guided down through a perforated aluminum tube, one and one-quarter inches in diameter. Fig. 3 shows a photograph of the valve and closure system. In Appendix G, calculations are provided which were used to estimate the closure time of the valve. The closure time of the valve was measured with an oscilloscope and a Polaroid camera. The

time sweep was triggered with a photoelectric cell. The closure was marked by a 45 volt direct current signal on the vertical plates of the oscilloscope. The distance that the sweep moved on the oscilloscope from trigger to closure, was photographed with 3000 speed Polaroid film. The closure time for the seven pound weight from nine feet was $0.007 \pm 0.003$ seconds. This agrees closely with the values calculated in Appendix G.

A Kistler model 401 quartz pressure transducer was installed at three locations along the pipe. A Kistler 407-5 low noise cable was used to connect the transducer to the Kistler model 651 piezo-calibrator amplifier. A shielded cable was used to connect the output of the piezo-calibrator amplifier to a Hewlett Packard model 130 oscilloscope. An oscilloscope Polaroid camera was used with Polaroid 3000 speed film to take a time exposure of the pressure-time history for each run. When the valve was completely closed, a 45 volt direct current circuit was completed. This triggered the oscilloscope time sweep. Fig. 4 is a photograph of the component parts of the pressure recording system.

## 4. Procedure.

The objective of the experimental part of this work was to verify the applicability of the theoretical model.

The pressure-time history was recorded at three locations along the pipe. Fig. 13 shows these locations. They were numbered starting from the valve, one, two, and three respectively. The pressure-time history was recorded at each transducer location for five different air-water mixtures at each nominal head in the head tank of two, four, six and eight feet. Since the effect of small amounts of air was of interest, air rates were chosen such that the volume percent air in the system was always less than ten percent.

Because of the effect of as little as 0.1 percent by volume air in the water for the no air runs, it was difficult to get good results with water taken directly from the water main. For these runs, it was found that better results were obtained if the water was left in the tank overnight.

The transducer was calibrated using an Ashcroft dead-weight tester. The calibration curves are given in Appendix C, Fig. 15 and 16.

A calibration curve for the rotometer was available from the manufacturer. Four points on this curve were checked with a positive displacement wet gas meter. The points checked closely, and the curve was used.

The detailed procedure for each run is given in Appendix D and a sample data sheet is shown in Appendix E.

Only one pressure transducer was used. This transducer was moved to the desired location for each run.

5. Results.

The results have been presented in the form of tables, photographs, and curves. In Table 1 "transducer locations" are numbered as shown in Appendix A, Fig. 13. The "head" refers to the head of water in the head tank. The values given are nominal, and the exact values of the heads are shown in Appendix A, Fig. 13. The term $\eta$ is the volume percent of air at the water inlet conditions of temperature and pressure. The term $\eta_{WT}$ is the weight percent of air in the mixture. P is the maximum pressure rise above the static pressure with no flow in the pipe. The ratio $P/P_{NT}$ is the ratio of the maximum pressure obtained when the valve is closed to the theoretical maximum pressure with no air, equation (4).

Results are tabulated for transducer locations one and two. Meaningful results were unattainable from location three. The reasons for this will be discussed later.

Fig. 6 shows a series of photographs for nominal heads of two and four feet of water and Fig. 7 shows the series of photographs for nominal heads of six and eight feet of water. Each row of photographs is for a given head. In the first photograph no air was injected into the water. The amount of air increases moving from left to right. The camera used to take the photographs takes the pictures such that the sweep of the oscilloscope moves from right to left rather than left to right as the oscilloscope sweep actually moves. The initial point in Fig. 6 and 7 has been marked by lines. The horizontal arrows point in the direction that the sweep moves along the horizontal scale. The vertical arrows point in the direction of increasing pressure. In the photographs, it should be noted that the pressure and time scales are different when air is injected from those when no air is injected.

In Fig. 8 through 11, the volume percent of air was based upon the water conditions of temperature and pressure at the inlet to the main run of pipe. Fig. 8, 9, 10, and 11 are respectively for nominal heads of two, four, six and eight feet of water. Both the theoretical adiabatic (Equation (6a)) and theoretical isothermal (Equation (6)) curves have been drawn in. The experimental points for transducer locations one and two are plotted and marked with symbols.

## 6. Discussion of Results.

Transducer location three could not be used to obtain meaningful data because the valve could not close fast enough. The valve would have had to close in less than 0.0015 seconds to get the maximum pressure without interference of the reflected pulse returning from the tank. Hence, only data from transducer locations one and two are presented. This subject was previously discussed in the theory section.

As the tabulated results show, two runs were made for each set of run conditions. This was done as a means of checking the accuracy and consistency of the results.

The weight percent of air in the two phase water-air mixture is included in the tabulated results to show the small weight fraction of air present in the air-water mixtures.

It was impossible to obtain meaningful results at transducer location one with no air in the water. The high frequency pressure pulses set up by the valve stem and gate vibrating made it impossible to distinguish between the pulse created by stopping the water and that created by the vibrating valve parts. With a small amount of air, these high frequency pulses were damped out and meaningful results were obtained. The effect of air in damping the high frequency noise is seen in Fig. 6 and 7.

The pressure-time photographs of Fig.6 and 7 show how the pressure-time history at transducer location two appeared on the oscilloscope. The photographs show that in the region observed; 1) the greater the percent of air present in the mixture, the smaller the pressure amplitude and the slower the pressure pulse moves down the pipe. The slowing rate of the pressure pulse is shown by the increasing time duration of the pulse as the air percent increases. 2) Small amounts of air have a large effect in

reducing the amplitude of the pressure pulse and in decreasing the pressure pulse speed.

The photographs taken at transducer location one show the same effects as the photographs taken at transducer location two. As a result, the photographs taken at transducer location one are not included in this report. Fig. 6 and 7 show the photographs taken at transducer location two. The results taken from the photographs are tabulated in Table 1.

In Fig. 8 through 11, the theoretical curves include no frictional losses. Because there are no frictional losses included in the theoretical curves, it would be expected that the experimental results should fall slightly below the theoretical curve. This is because the frictional losses for a two phase mixture are greater than those for a single phase. Martinelli experimentally showed this. /10/ As discussed in the theory section, the compression of the air by the pressure pulse was probably best described as adiabatic because the method of injection allowed for large bubbles which gave a small heat transfer area per unit volume. The pressure pulse travels so fast that the air is compressed for a very short time, consequently this permits very little time for heat transfer.

For the runs when no air was injected into the water, values of 81.7, 71.7, 74.7 and 79.9 percent of the theoretical maximum pressure were obtained at transducer location two for nominal heads of two, four, six, and eight feet respectively. Entrained air in the water of about 0.02 percent by volume would cause this effect. The entrained air was under pressure of about 100 psia in the United States Naval Postgraduate School system. When the water pressure was reduced, the air expanded and the volume percent increased. A glass of water will have air bubbles on the glass surface if allowed to sit overnight.

By allowing the water to stand about fifteen hours in the tank, the maximum pressure obtained when no air was injected increased from approximately 50 percent to about 80 percent of the theoretical maximum. This indicates that the runs in which no air was injected had enough entrained air in the water that the exact air content was uncertain. A factor of 0.02 percent by volume makes a large difference in the maximum pressure obtained in the region approaching zero percent of air. This same percent of uncertainty makes very little difference in the maximum pressure in the region greater than about 0.5 percent of air. Therefore, this entrained air did not effect the results appreciably for values greater than 0.5 percent of air.

The curves of Fig. 8 through 12 were plotted on a scale in which the low ranges of pressure and volume percent were expanded. This was done to better show the region of greatest change. A log scale was used in which for the ordinate ln ( $P/P_{NT}$ + 0.1) was plotted and for the abscissa ln ( $\eta$ + 1.0) was plotted. This was done so that it would be possible to have zeros for $P/P_{NT}$ and $\eta$ on the scales. The results indicate that the points fall close to the theoretical curves in the regions greater than two percent of air. In the region of less than two percent of air, the results obtained are more erratic. The uncertainty in the region of 0.5 percent by volume air was plus or minus about ten percent in the volume percent term, and about plus or minus 11.0 percent in the $P/P_{NT}$ term. Even considering these uncertainties, several of the points in the region less than two percent by volume air do not fall on the theoretical curve. In the region of greater than two percent by volume air the consistency of the data was much better. At four percent by volume air, the uncertainty of the volume percent term ($\eta$) was about plus or minus 0.8 percent and that of the $P/P_{NT}$

term was about plus or minus 17.0 percent. These uncertainties are based upon the uncertainty analysis of runs 3-9-2 and 3-9-10 given in Appendix H.

Fig. 12 shows the effect of air in damping pressure pulses in systems at pressure up to 500 psia. This figure shows curves of $(P/P_{NT})_T$ vs $\eta$ for pressures of 500, 400, 300, 200, 100, and 15.5 psia. The volume percent of air at inlet conditions varies from zero to ten percent. These curves show that the lower the pressure in which the pressure pulse is being transmitted, the greater is the effect of air in reducing the pressure amplitude. As an example, at one percent by volume of air at 15.5 psia, the pressure would be reduced to 8.6 percent of the original pressure. At 100, 200, 300, 400, and 500 psi the pressure amplitude reduction would be to 20.8, 28.7, 34.4, 38.9, and 42.5 percent respectively of the original pressure amplitude.

As an example of the usefulness of air in reducing pressure pulses and also to get an idea of the amount of air that would be required, consider the following example.

Example 1. Pure water is flowing through a two inch extra strong pipe at the rate of 500 gpm. The system has an operating pressure of 100 psia and an operating temperature of 70°F. Fluid borne noises are being transmitted in this system. It is desired to reduce the amplitude of these pressure pulses to 20 percent of the original amplitude.

Fig. 12 shows that for the pressure amplitude to be 20 percent of the original amplitude, a 1.05 percent by volume mixture must be made by the injection of air.

$$\frac{500 \text{ gpm}}{7.48 \text{ gal/ft}^3} = 66.84 \text{ ft}^3/\text{min water}$$

Let x equal the air required in $ft^3$/min at 100 psia and 70°F.

Then

$$0.0105 = \frac{100X}{X + 66.84}$$

x = 0.7093 $ft^3$/min at 100 psia and 70°F

This equals 4.825 $ft^3$/min at 14.7 psia and 70°F.

The weight of air required would be 0.3628 lbm/min.

## 7. Conclusions.

Based upon the experimental work and development of equations (6) and (6a) the following conclusions have been made.

1. Small amounts of air in a water system greatly reduce the amplitude of a pressure pulse transmitted in the water. In a 15.5 psia water system with one percent by volume air, the pressure is reduced to 8.6 percent of the theoretical no-air amplitude.

2. The effect of air in damping pressure pulses decreases as the pressure of the system increases as demonstrated by Fig. 12.

3. There was a reasonable correlation of experimental results with theory as shown in Fig. 8 through 11.

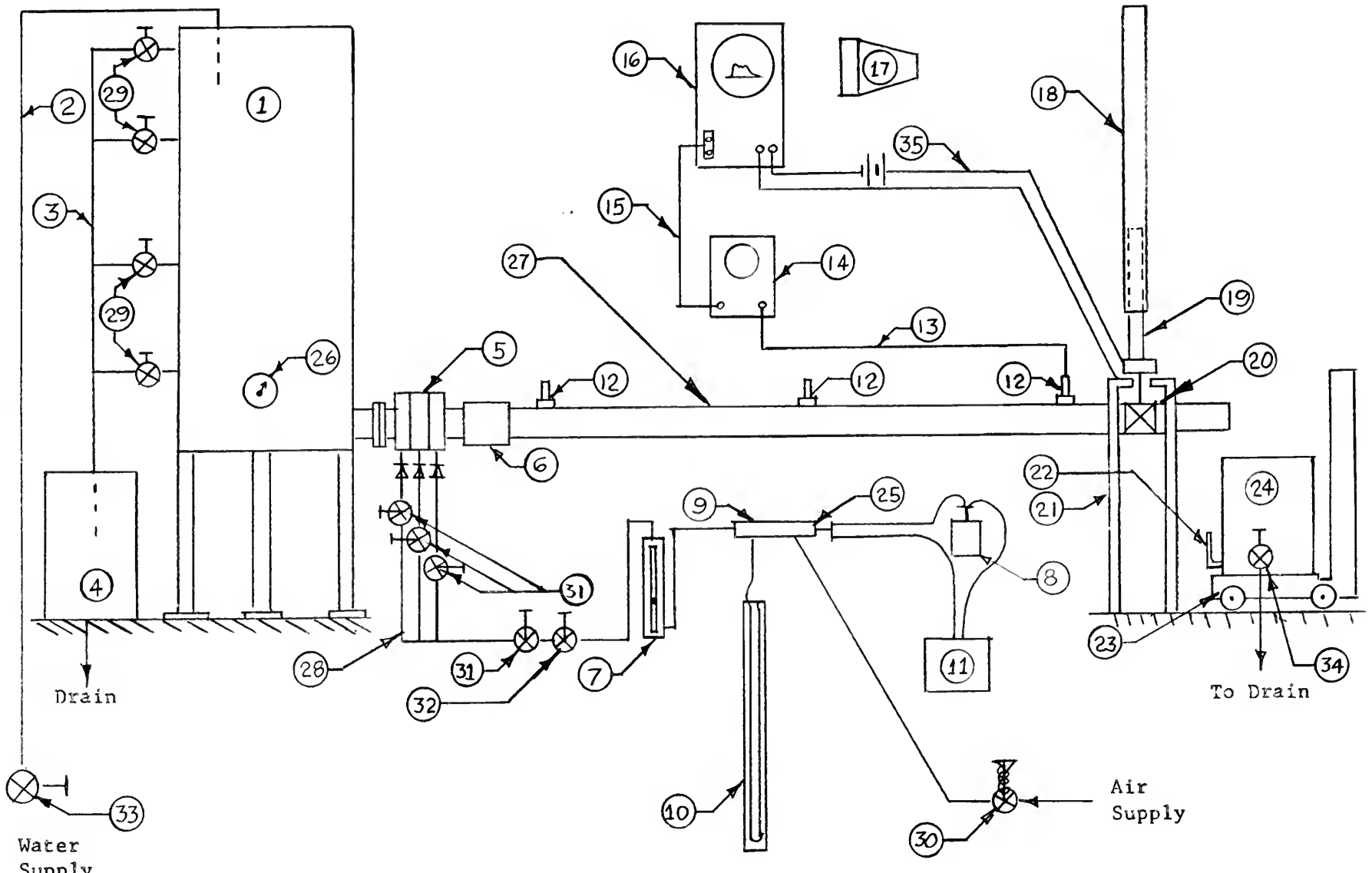


Fig. 1 System Diagram

KEY TO SYSTEM DIAGRAM

1. Water storage tank
2. Two inch water fill line
3. Storage tank overflow piping system
4. Overflow drain tank
5. Air injection system
6. Two inch pipe coupling
7. Fischer and Porter rotometer
8. Potentiometer reference ice bath
9. Air manifold
10. Inlet air mercury manometer
11. Thermocouple potentiometer
12. Kistler Model 401 piezoelectric pressure transducer
13. Kistler #470 shielded cable
14. Kistler Model #651 piezo-calibrator
15. Shielded calibrator-oscilloscope cable
16. Hewlett Packard Model 130 oscilloscope
17. Polaroid oscilloscope camera
18. Falling weight guide tube
19. Seven pound weight
20. Modified Crane two inch quick closing valve
21. Quick closing valve stop
22. Water discharge mercury thermometer
23. Dayton scales
24. Weigh tank
25. Air inlet themocouple

26. Water inlet Weston thermometer

27. Standard ASA two inch extra strong steel pipe

28. One quarter inch vinyl tubing

29. Two inch gate valves

30. Air regulating valve

31. Quick closing air stop valve

32. Air flow regulating valve

33. Water inlet regulating valve

34. Weigh tank two inch discharge gate valves

35. Oscilloscope sweep trigger

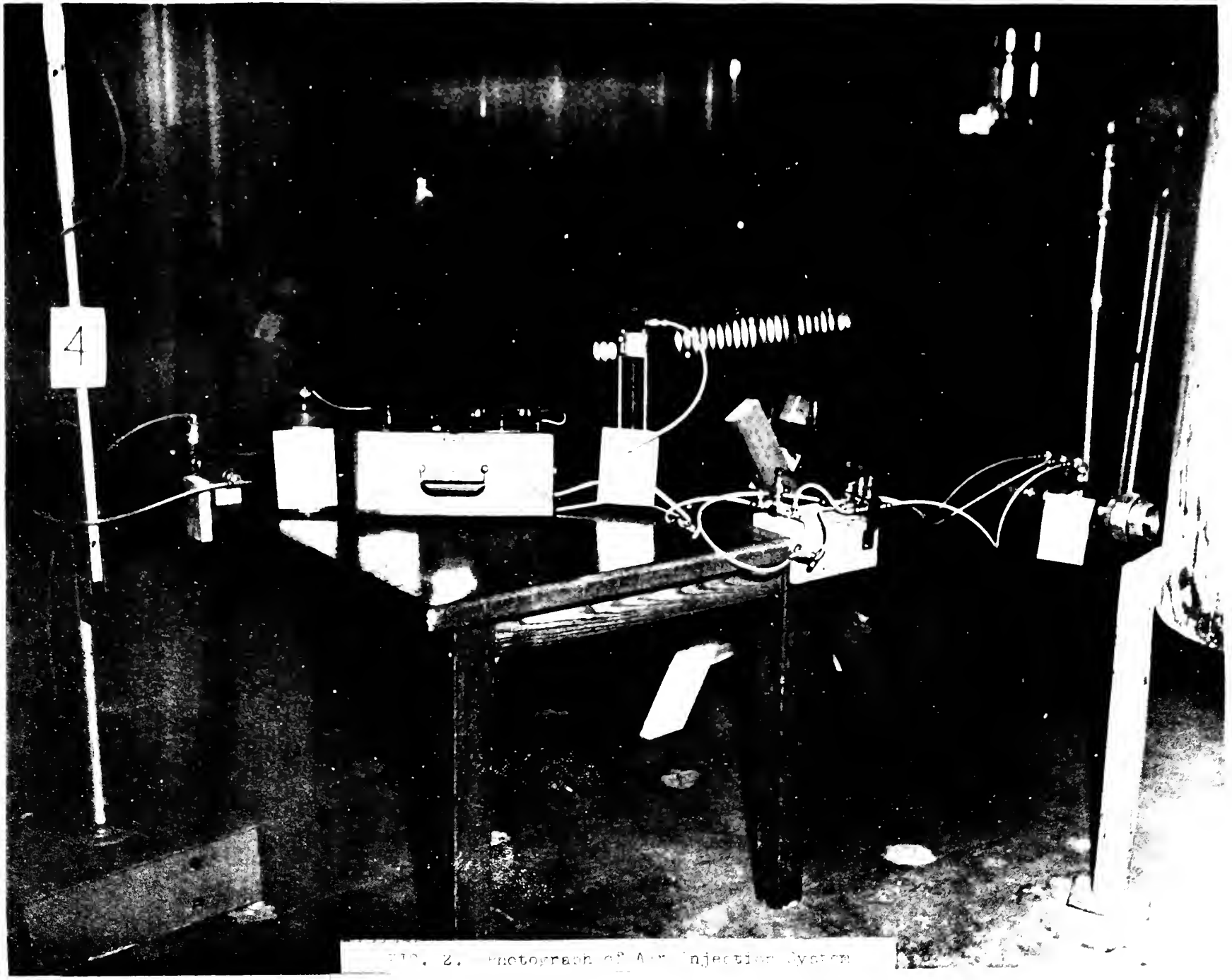


FIG. 2. Photograph of Air Injection System

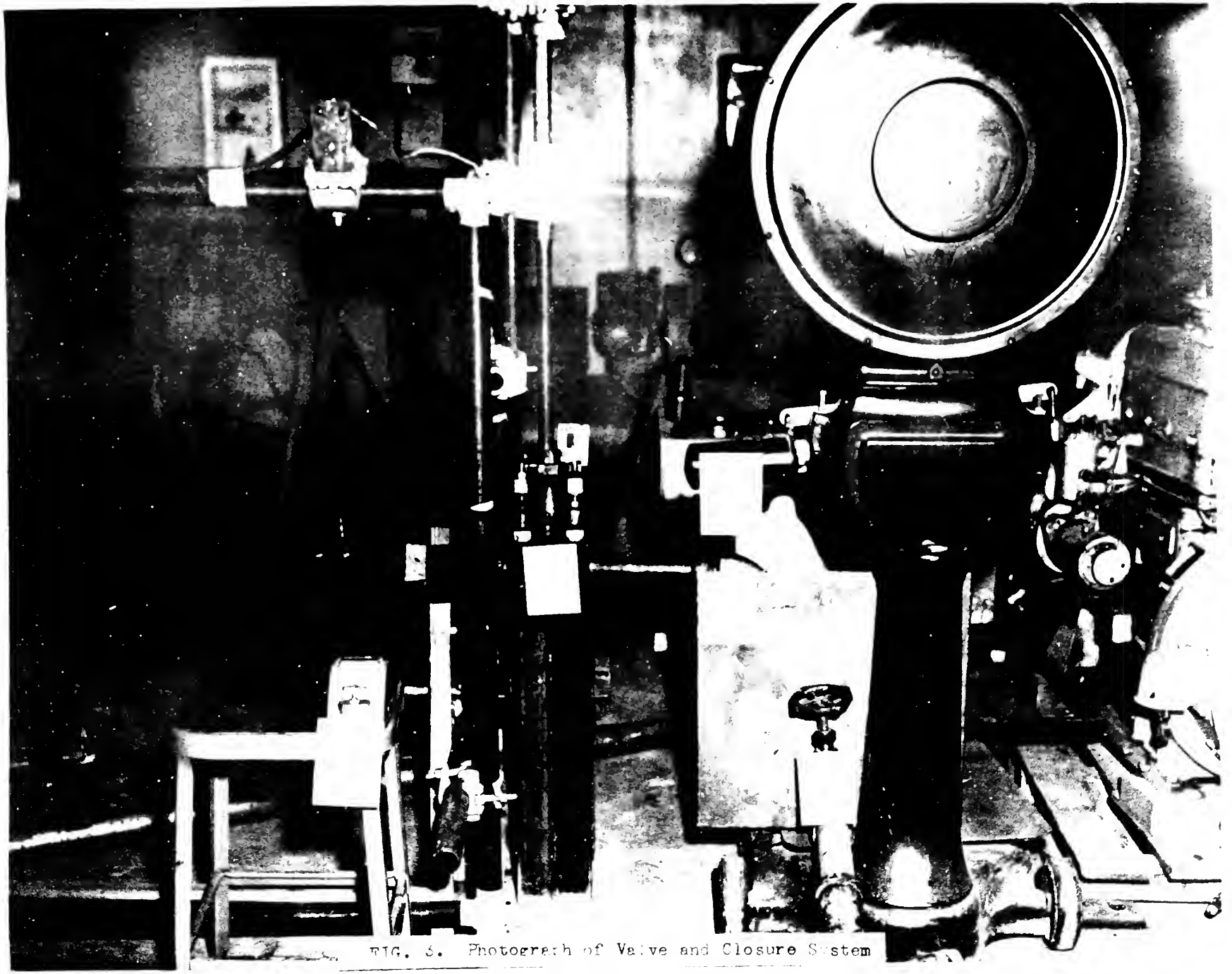

FIG. 5. Photograph of Valve and Closure System

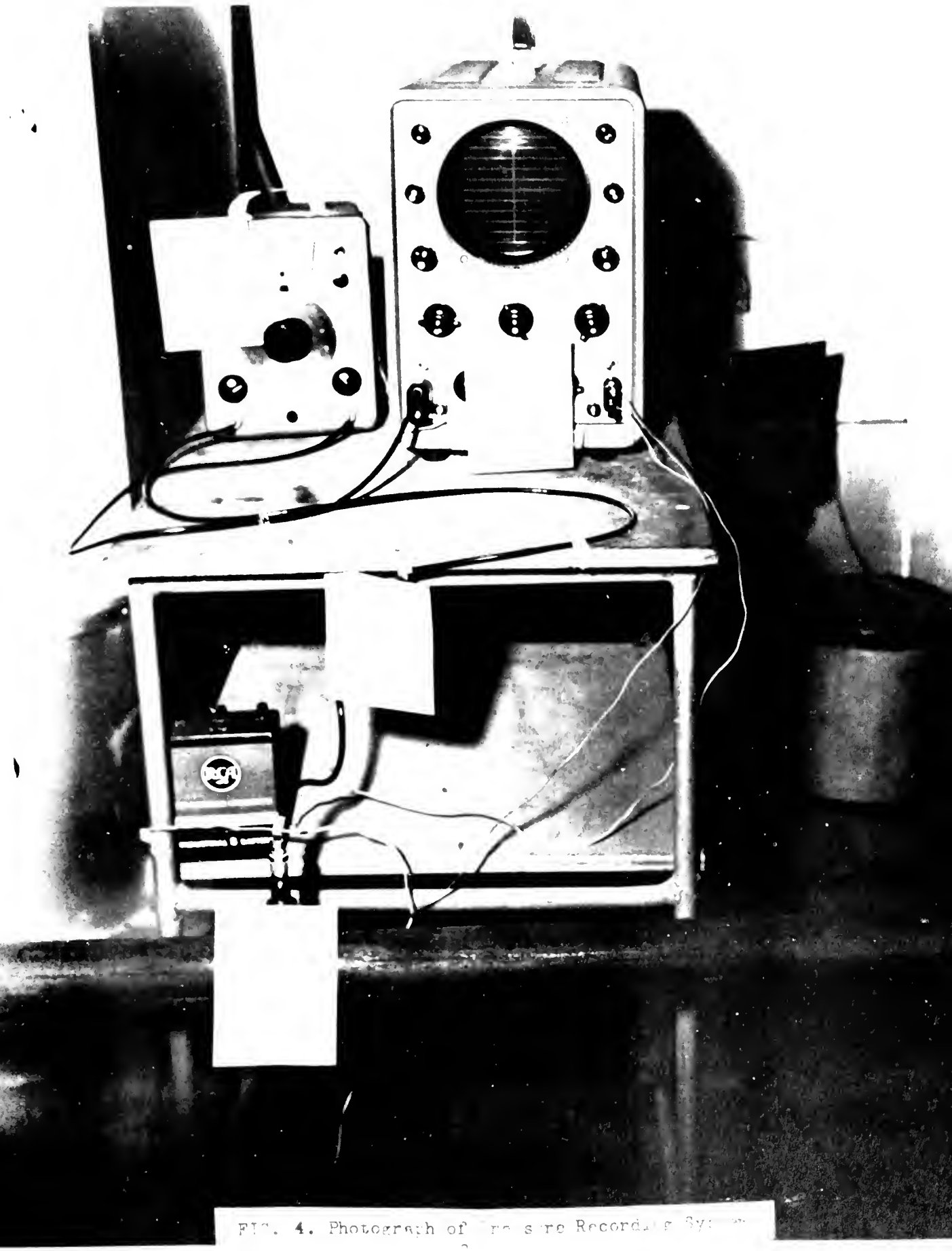

FIG. 4. Photograph of [illegible] Recorder System

KEY TO EQUIPMENT PHOTOGRAPHS

| Item | Description |
|---|---|
| 1. | Thermocouple potentiometer |
| 2. | Fisher and Porter rotometer |
| 3. | Potentiometer reference ice bath |
| 4. | Inlet air mercury manometer |
| 5. | Air injection system |
| 6. | Hewlett Packard model 130 oscilloscope |
| 7. | Kistler model #651 piezo-calibrator |
| 8. | Kistler #470 shielded cable |
| 9. | Kistler model 401 piezo-electric pressure transducer |
| 10. | Modified Crane quick closing valve |
| 11. | Falling weight guide tube with weight in it |
| 12. | Weigh tank |
| 13. | Dayton scales |
| 14. | Weigh tank discharge valve |
| 15. | Electric timer |

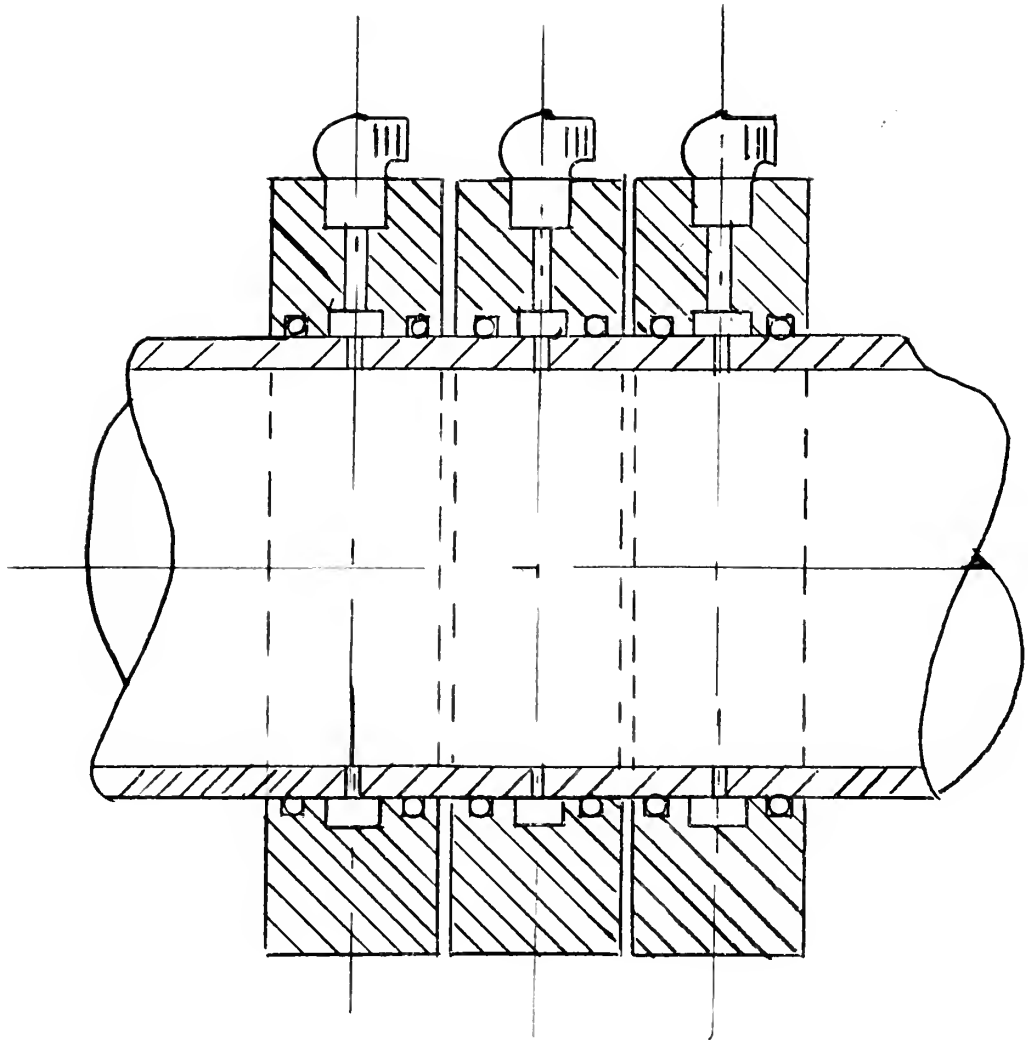

Fig. 5 Cross Sectional View of Air Injection Annular Ring

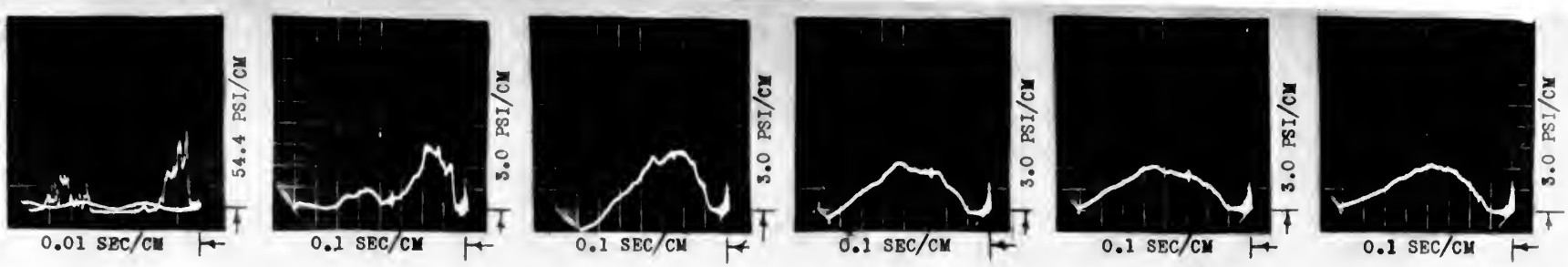


| | | | | | | |
|---|---|---|---|---|---|---|
| RUN NO. | 3-27-4 | 2-28-4 | 2-28-13 | 2-28-16 | 2-28-17 | 2-28-19 |
| HEAD, ft. | 2 | 2 | 2 | 2 | 2 | 2 |
| $\eta$, % | 0 | 1.20 | 3.13 | 5.18 | 7.20 | 9.54 |
| $\eta_{WT}$, % | 0 | 0.00165 | 0.00425 | 0.00722 | 0.0102 | 0.01387 |
| LOCATION | 2 | 2 | 2 | 2 | 2 | 2 |



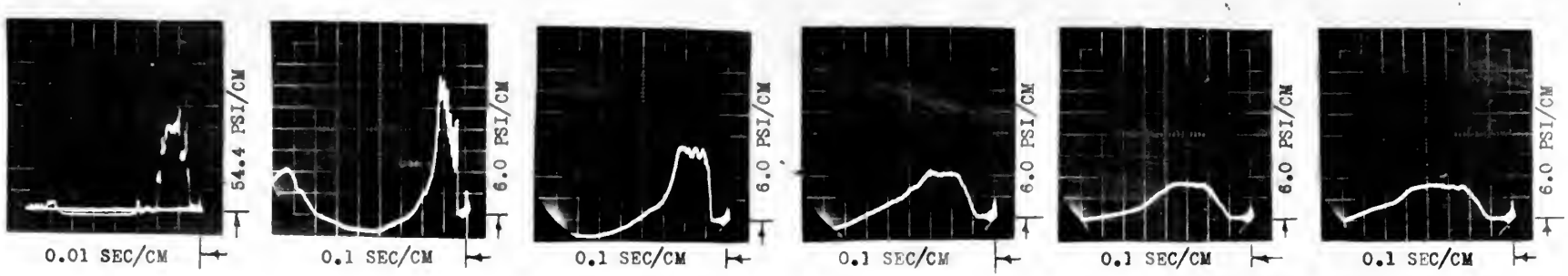


| | | | | | | |
|---|---|---|---|---|---|---|
| RUN NO. | 3-27-3 | 2-28-26 | 2-28-28 | 2-28-30 | 2-28-32 | 2-28-34 |
| HEAD, ft. | 4 | 4 | 4 | 4 | 4 | 4 |
| $\eta$, % | 0 | 0.769 | 2.09 | 3.49 | 5.02 | 6.24 |
| $\eta_{WT}$, % | 0 | 0.00111 | 0.00312 | 0.00518 | 0.00755 | 0.00951 |
| LOCATION | 2 | 2 | 2 | 2 | 2 | 2 |

One division on the photographs equals one centimeter

FIG. 6 PRESSURE- TIME PHOTOGRAPHS PART 1.

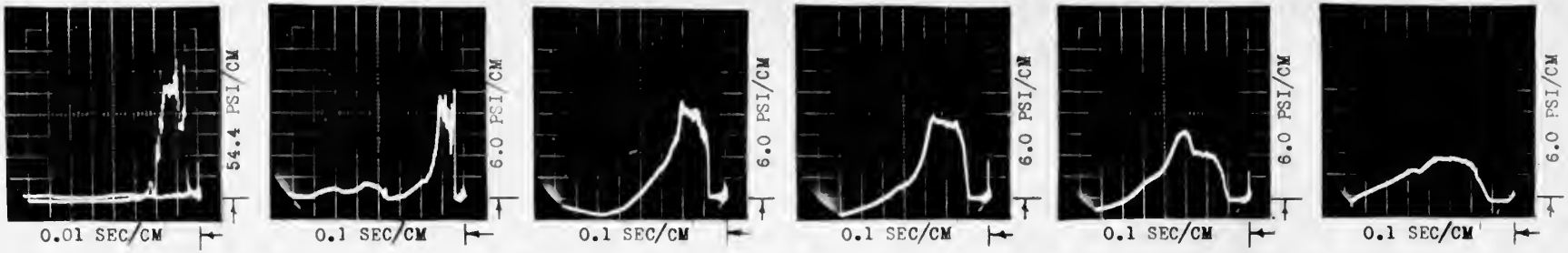


| RUN NO. | 3-27-2 | 3-3-4 | 3-3-7 | 3-3-8 | 3-3-10 | 3-3-13 |
|---|---|---|---|---|---|---|
| HEAD, ft. | 6 | 6 | 6 | 6 | 6 | 6 |
| $\eta$, % | 0 | 0.596 | 1.59 | 2.59 | 3.62 | 4.76 |
| $\eta_{WT}$, % | 0 | 0.000877 | 0.00241 | 0.00390 | 0.00551 | 0.00732 |
| LOCATION | 2 | 2 | 2 | 2 | 2 | 2 |



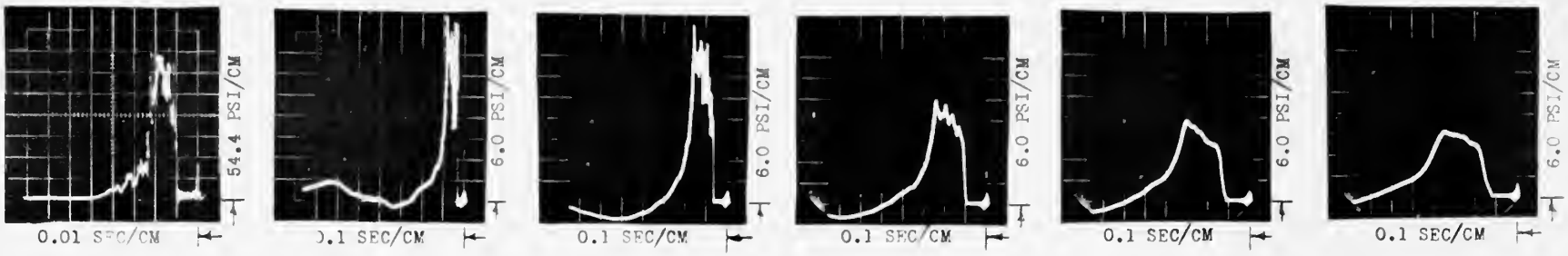


| RUN NO. | 3-27-1 | 3-9-2 | 3-9-5 | 3-9-7 | 3-9-9 | 3-9-10 |
|---|---|---|---|---|---|---|
| HEAD | 8 | 8 | 8 | 8 | 8 | 8 |
| $\eta$, % | 0 | 0.485 | 1.26 | 2.15 | 3.01 | 3.89 |
| $\eta_{WT}$, % | 0 | 0.000750 | 0.00212 | 0.00345 | 0.00476 | 0.00637 |
| LOCATION | 2 | 2 | 2 | 2 | 2 | 2 |

One division of the photograph ths equals one centi[illegible]

FIG. 7 PRESSURE-TIME PHOTOGRAPHS PART 2.

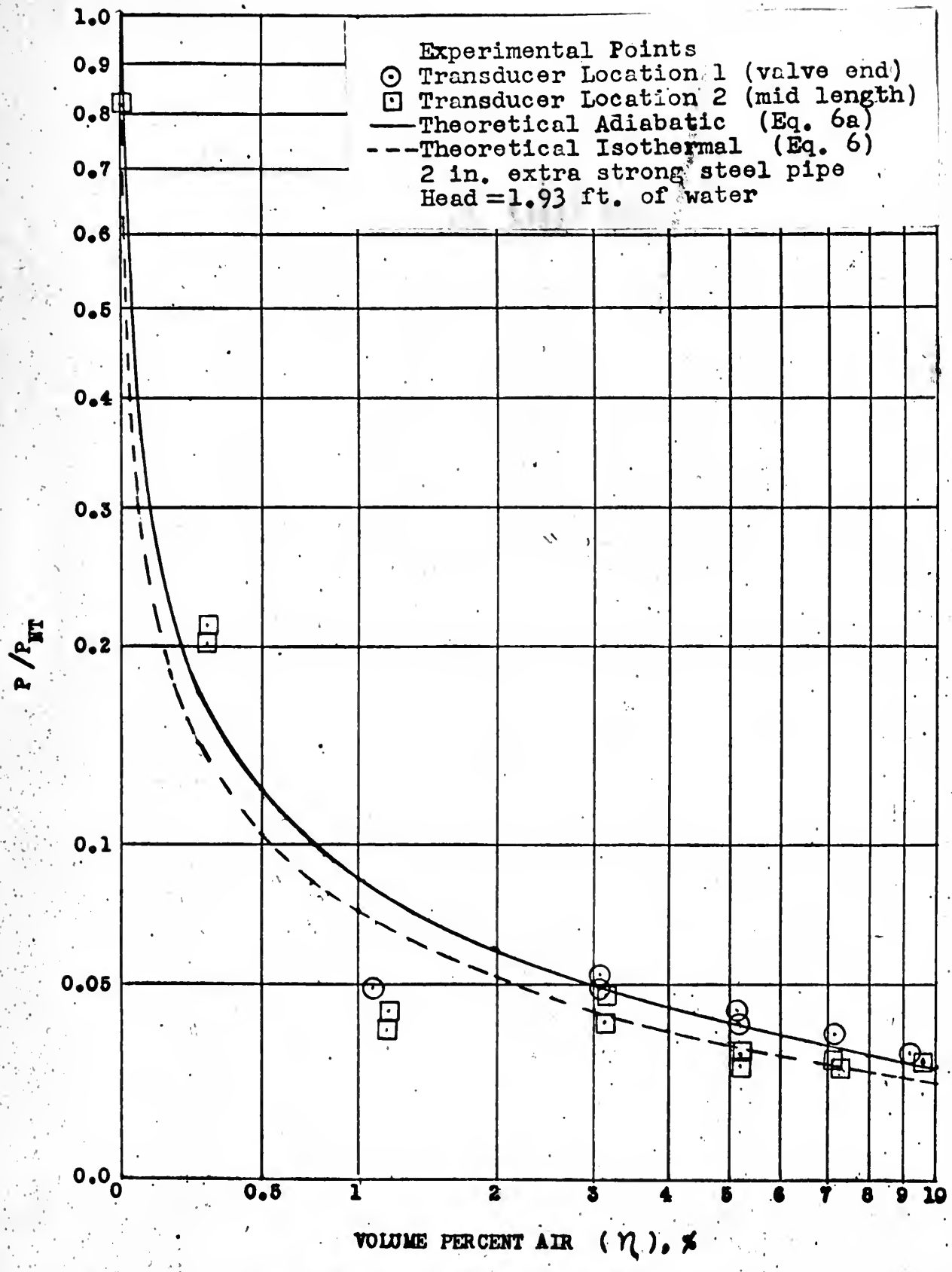


FIG. 8 $P/P_{NT}$ vs. $\eta$, HEAD TWO FEET

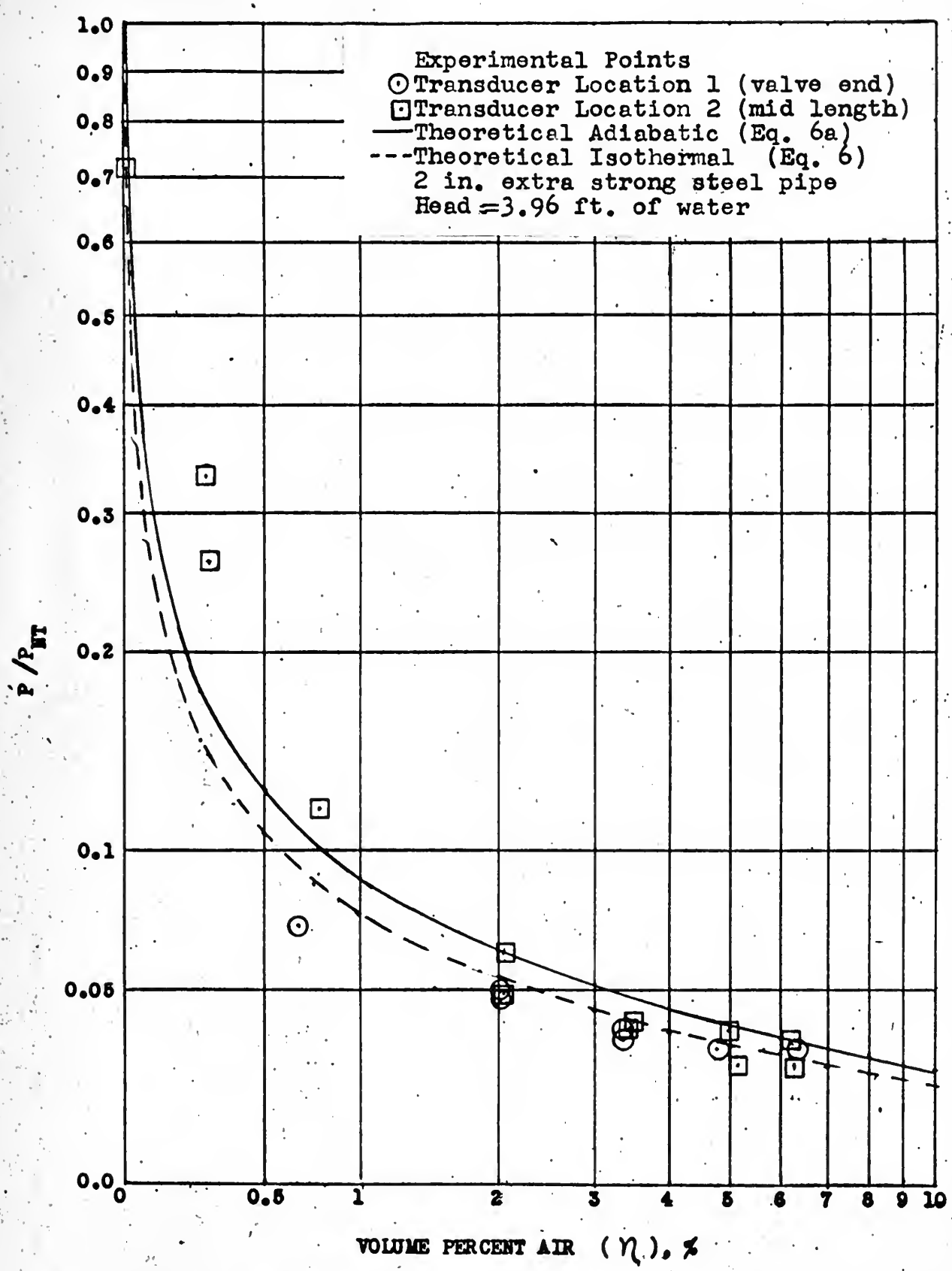


FIG. 9 $P/P_{NT}$ vs. $\eta$, HEAD FOUR FEET

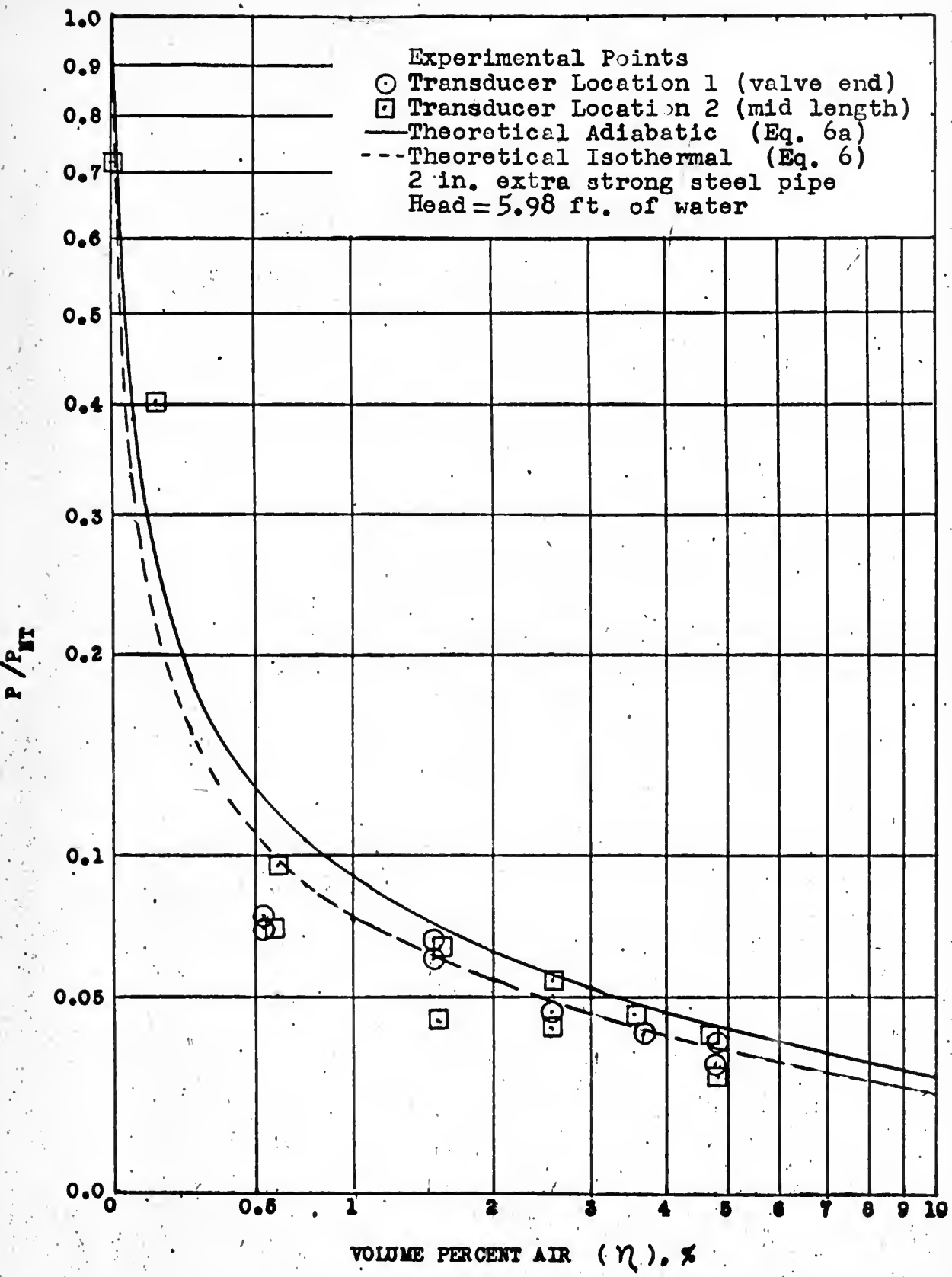


FIG. 10 $P/P_{NT}$ vs. $\eta$, HEAD SIX FEET

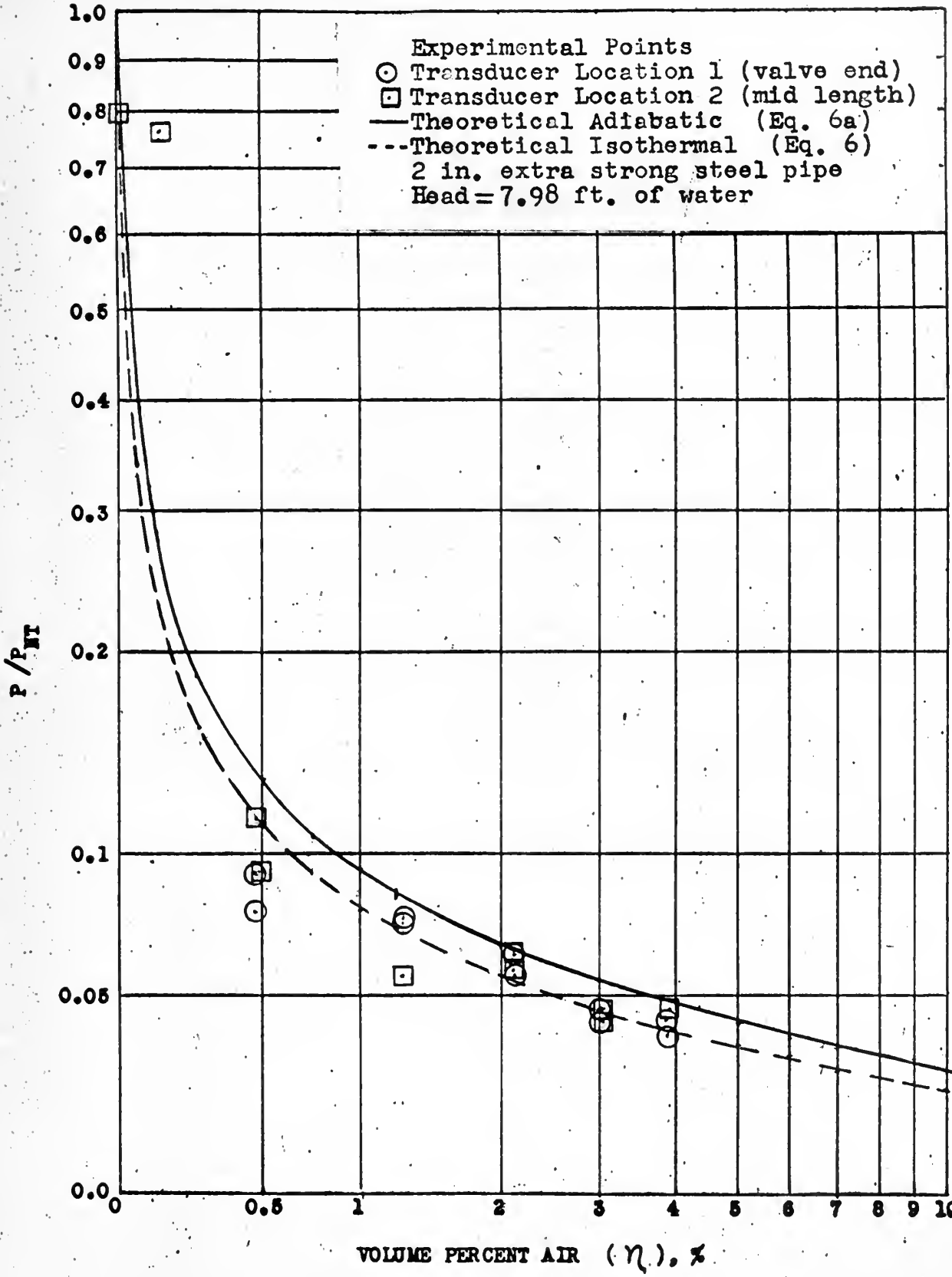


FIG. 11 $P/P_{NT}$ vs. $\eta$, HEAD EIGHT FEET

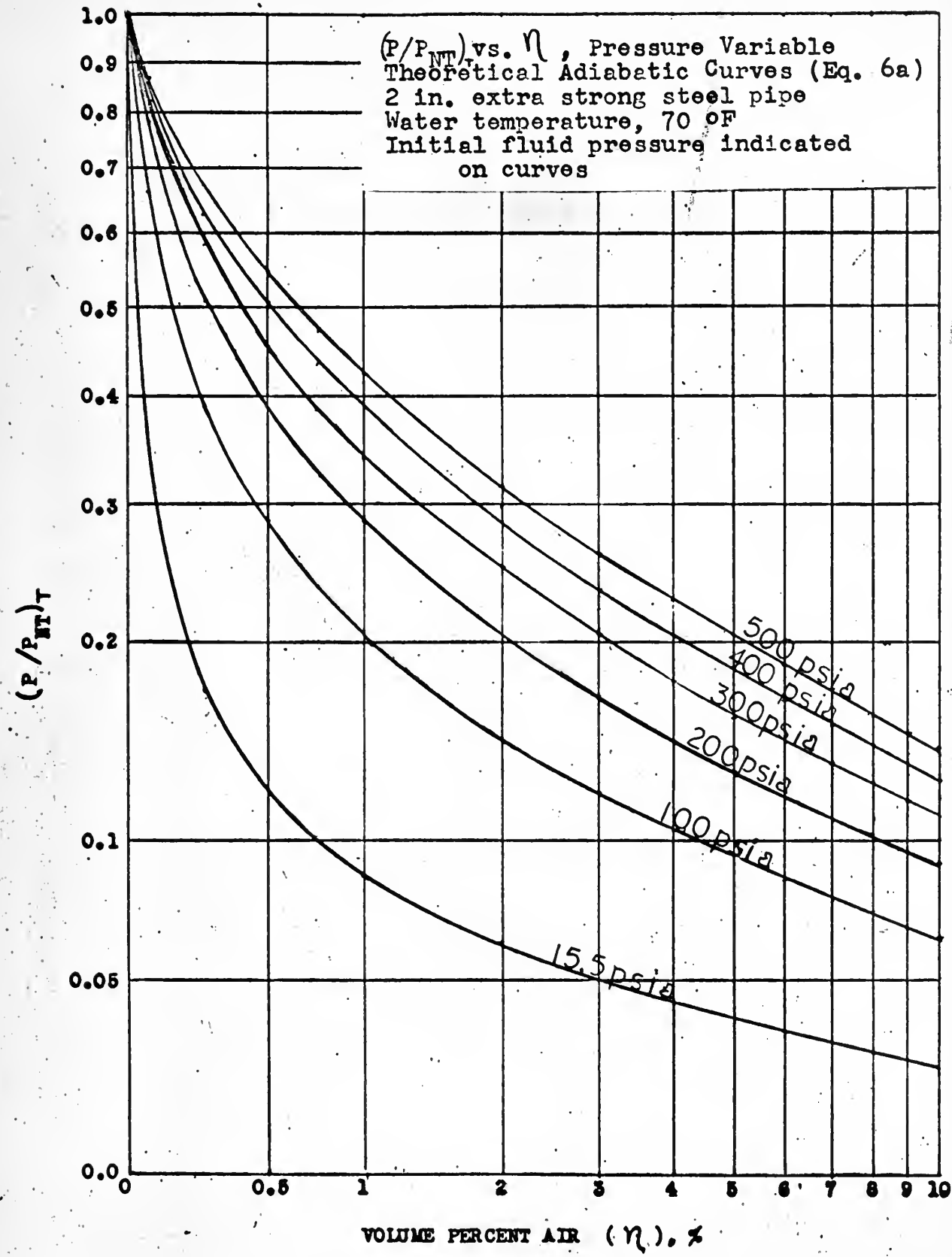


FIG. 12 $(P/P_{NT})_T$ VS. $\eta$, PRESSURE VARIABLE

Table 1. Tabulated Results

| Run No. | Transducer Location | Head ft. | $\eta$ % | $\eta_{WT}$ %x10$^{-3}$ | P psi | $P/P_{NT}$ |
|---|---|---|---|---|---|---|
| 3-21-32 | 1 | 2 | 1.09 | 1.42 | 10.6 | 0.0498 |
| 3-21-33 | 1 | 2 | 1.09 | 1.42 | 10.6 | 0.0498 |
| 3-21-34 | 1 | 2 | 3.05 | 4.08 | 10.6 | 0.0498 |
| 3-21-35 | 1 | 2 | 3.10 | 4.14 | 11.2 | 0.0526 |
| 3-21-36 | 1 | 2 | 5.14 | 7.02 | 8.8 | 0.0413 |
| 3-21-37 | 1 | 2 | 5.17 | 7.06 | 8.2 | 0.0385 |
| 3-21-38 | 1 | 2 | 7.19 | 10.05 | 7.3 | 0.0343 |
| 3-21-39 | 1 | 2 | 7.19 | 10.04 | 7.3 | 0.0343 |
| 3-21-40 | 1 | 2 | 9.23 | 13.16 | 6.4 | 0.0300 |
| 3-21-41 | 1 | 2 | 9.28 | 13.23 | 6.4 | 0.0300 |
| 3-21-18 | 1 | 4 | 0.664 | 1.83 | 22.4 | 0.0704 |
| 3-21-19 | 1 | 4 | 0.664 | 1.83 | 22.4 | 0.0704 |
| 3-21-20 | 1 | 4 | 2.02 | 2.83 | 14.6 | 0.0462 |
| 3-21-21 | 1 | 4 | 2.01 | 2.80 | 15.8 | 0.0497 |
| 3-21-22 | 1 | 4 | 3.37 | 4.78 | 11.1 | 0.0349 |
| 3-21-23 | 1 | 4 | 3.37 | 4.77 | 11.9 | 0.0374 |
| 3-21-25 | 1 | 4 | 4.77 | 6.85 | 10.4 | 0.0327 |
| 3-21-26 | 1 | 4 | 6.38 | 9.31 | 10.4 | 0.0327 |
| 3-21-27 | 1 | 4 | 6.38 | 9.31 | 10.4 | 0.0327 |
| 3-21-3 | 1 | 6 | 0.538 | 0.774 | 30.6 | 0.0765 |
| 3-21-4 | 1 | 6 | 0.536 | 0.769 | 28.8 | 0.0720 |
| 3-21-5 | 1 | 6 | 1.53 | 2.23 | 26.4 | 0.0660 |
| 3-21-6 | 1 | 6 | 1.53 | 2.23 | 24.6 | 0.0615 |

Table 1. Tabulated Results (continued)

| Run No. | Transducer Location | Head ft. | $\eta$ % | $\eta_{WI}$ %x10$^{-3}$ | P | P/P$_{NT}$ |
|---|---|---|---|---|---|---|
| 3-21-7 | 1 | 6 | 2.60 | 3.84 | 18.0 | 0.0450 |
| 3-21-8 | 1 | 6 | 2.60 | 3.84 | 18.0 | 0.0450 |
| 3-21-13 | 1 | 6 | 3.68 | 5.49 | 15.6 | 0.0390 |
| 3-21-14 | 1 | 6 | 3.68 | 5.49 | 15.6 | 0.0390 |
| 3-21-15 | 1 | 6 | 4.76 | 7.18 | 12.0 | 0.0300 |
| 3-21-16 | 1 | 6 | 4.80 | 8.07 | 14.4 | 0.0360 |
| 3-13-3 | 1 | 8 | 0.475 | 0.731 | 35.8 | 0.0773 |
| 3-13-4 | 1 | 8 | 0.475 | 0.731 | 41.7 | 0.0901 |
| 3-13-5 | 1 | 8 | 1.28 | 2.04 | 33.5 | 0.0724 |
| 3-13-6 | 1 | 8 | 1.28 | 2.01 | 34.6 | 0.0747 |
| 3-13-7 | 1 | 8 | 2.14 | 3.35 | 25.7 | 0.0555 |
| 3-13-8 | 1 | 8 | 2.14 | 3.35 | 29.3 | 0.0633 |
| 3-13-9 | 1 | 8 | 3.01 | 4.77 | 19.1 | 0.0413 |
| 3-13-10 | 1 | 8 | 3.01 | 4.77 | 20.9 | 0.0451 |
| 3-13-11 | 1 | 8 | 3.91 | 6.22 | 17.9 | 0.0387 |
| 3-13-12 | 1 | 8 | 3.91 | 6.22 | 19.1 | 0.0413 |
| 2-27-4 | 2 | 2 | 0 | 0 | 174.0 | 0.817 |
| 4-1-4 | 2 | 2 | 0.294 | 0.382 | 43.1 | 0.202 |
| 4-1-5 | 2 | 2 | 0.294 | 0.382 | 45.4 | 0.213 |
| 2-28-4 | 2 | 2 | 1.20 | 1.65 | 8.68 | 0.0410 |
| 2-28-5 | 2 | 2 | 1.19 | 1.58 | 7.78 | 0.0365 |
| 2-28-13 | 2 | 2 | 3.13 | 4.25 | 8.07 | 0.0379 |
| 2-28-14 | 2 | 2 | 3.10 | 4.22 | 9.97 | 0.0468 |

Table 1 Tabulated Results (continued)

| Run No. | Transducer Location | Head ft. | $\eta$ % | $\eta_{WT}$ %x10$^{-3}$ | P | $P/P_{NT}$ |
|---|---|---|---|---|---|---|
| 2-28-15 | 2 | 2 | 5.20 | 7.23 | 5.67 | 0.0266 |
| 2-28-16 | 2 | 2 | 5.18 | 7.22 | 6.27 | 0.0294 |
| 2-28-17 | 2 | 2 | 7.20 | 10.2 | 6.03 | 0.0283 |
| 2-28-18 | 2 | 2 | 7.28 | 10.1 | 5.37 | 0.0252 |
| 2-28-19 | 2 | 2 | 9.54 | 13.9 | 5.97 | 0.0280 |
| 3-27-3 | 2 | 4 | 0 | 0 | 228 | 0.717 |
| 4-1-6 | 2 | 4 | 0.277 | 0.257 | 105.3 | 0.331 |
| 4-1-7 | 2 | 4 | 0.277 | 0.257 | 84.1 | 0.261 |
| 2-28-26 | 2 | 4 | 0.769 | 1.11 | 37.9 | 0.118 |
| 2-28-28 | 2 | 4 | 2.087 | 3.12 | 19.9 | 0.0626 |
| 2-28-29 | 2 | 4 | 2.087 | 3.12 | 15.7 | 0.0494 |
| 2-28-30 | 2 | 4 | 3.49 | 5.18 | 12.1 | 0.0380 |
| 2-28-31 | 2 | 4 | 3.51 | 5.20 | 12.7 | 0.0399 |
| 2-28-32 | 2 | 4 | 5.02 | 7.55 | 9.10 | 0.0286 |
| 2-28-33 | 2 | 4 | 4.99 | 7.48 | 12.1 | 0.0380 |
| 2-28-34 | 2 | 4 | 6.24 | 9.51 | 9.1 | 0.0286 |
| 2-28-25 | 2 | 4 | 6.20 | 9.67 | 10.9 | 0.0343 |
| 3-27-2 | 2 | 6 | 0 | 0 | 228.1 | 0.717 |
| 4-1-8 | 2 | 6 | 0.136 | 0.207 | 161.8 | 0.404 |
| 3-3-4 | 2 | 6 | 0.596 | 0.877 | 28.6 | 0.0715 |
| 3-3-5 | 2 | 6 | 0.602 | 0.893 | 38.8 | 0.0956 |
| 3-3-6 | 2 | 6 | 1.57 | 2.33 | 16.9 | 0.0422 |
| 3-3-7 | 2 | 6 | 1.59 | 2.41 | 26.2 | 0.0655 |
| 3-3-8 | 2 | 6 | 2.59 | 3.90 | 22.0 | 0.0550 |

Table 1 Tabulated Results (continued)

| Run No. | Transducer Location | Head ft. | $\eta$ % | $\eta_{WT}$ %x10$^{-3}$ | P | P/P$_{NT}$ |
|---|---|---|---|---|---|---|
| 3-3-9 | 2 | 6 | 2.58 | 3.89 | 16.0 | 0.0400 |
| 3-3-10 | 2 | 6 | 3.61 | 5.51 | 17.8 | 0.0445 |
| 3-3-11 | 2 | 6 | 3.61 | 5.51 | 17.8 | 0.0445 |
| 3-3-12 | 2 | 6 | 4.70 | 7.24 | 15.4 | 0.0385 |
| 3-3-13 | 2 | 6 | 4.76 | 7.32 | 10.6 | 0.0265 |
| 3-27-1 | 2 | 8 | 0 | 0 | 370 | 0.799 |
| 4-1-10 | 2 | 8 | 0.117 | 0.179 | 356.9 | 0.771 |
| 3-9-2 | 2 | 8 | 0.485 | 0.750 | 51.9 | 0.112 |
| 3-9-3 | 2 | 8 | 0.484 | 0.747 | 42.3 | 0.0913 |
| 3-9-5 | 2 | 8 | 1.26 | 2.12 | 48.9 | 0.106 |
| 3-9-6 | 2 | 8 | 2.13 | 3.41 | 26.7 | 0.0576 |
| 3-9-7 | 2 | 8 | 2.15 | 3.45 | 27.9 | 0.0602 |
| 3-9-8 | 2 | 8 | 3.01 | 4.76 | 19.5 | 0.0421 |
| 3 9-9 | 2 | 8 | 3.01 | 4.76 | 21.3 | 0.0460 |
| 3-9-10 | 2 | 8 | 3.89 | 6.37 | 17.1 | 0.0462 |
| 3-9-11 | 2 | 8 | 3.89 | 6.37 | 15.5 | 0.0462 |

## BIBLIOGRAPHY


1. Bergeron, L. T., Water Hammer in Hydraulics and Wave Surges in Electricity. John Wiley and Sons, Inc., 1961.

2. Fisher and Porter Company Catalog, Section 98-A. "Theory of the Flowrator", 1947.

3. Giles, R. V., Theory and Problems of Fluid Mechanics and Hydraulics., Schaum, 1962.

4. Karplus, H. B., The Velocity of Sound in a Liquid Containing Gas Bubbles, Armour Research Foundation; Project No. A-097, Atomic Energy Commission Contract No. AF (11-1)-528, United States Atomic Energy Commission, 1958.

5. Kistler Model 401, Quartz Pickup and Model 651 Amplifier, Kistler Instrument Corporation.

6. Kline, S. J., and F. A. McClintock. Describing Uncertainties in Single-Sample Experiments. Mechanical Engineering, 75, pp. 3-8, January 1953.

7. LeConte, J. N., Experiments and Calculations on Resurge Phase of Water Hammer, Transactions of the America. Society of Mechanical Engineers, 59-12 pp. 691-624, 1937.

8. Lieberman, P., Blast-Wave Propagation in Hydraulic Conduits. American Society of Mechanical Engineer's Paper No. 63-WA-125, 1963.

9. Leon, K. S., Instrumentation in Scientific Research. McGraw-Hill, 1959.

10. Martinelli, R. C., Isothermal Pressure Drop for Two Phase Two-Component Flow in a Horizontal Pipe. Transactions of the American Society of Mechanical Engineers, 66, pp. 139-151, February, 1944.

11. Operating and Servicing Manual for Model 130A Oscilloscopes, Hewlett-Packard Company, 1957.

12. Rich, C. R., Water-Hammer Analysis by the Laplace Mellin Transformation. Transactions of the American Society of Mechanical Engineers. pp. 361-368, July, 1945.

13. Stephanoff, A. J., Centrifugal and Axial Flow Pumps, 2nd Edition, John Wiley and Sons, Inc., 1957.

14. Sweeney, R. J., Measurement Techniques in Mechanical Engineering, John Wiley and Sons, Inc., 1953.

15. Swieciki, I., Rigid Water-Column Theory in Water Hammer Problems. American Society of Mechanical Engineers Paper No. 63-WA-80, 1963.

APPENDIX A

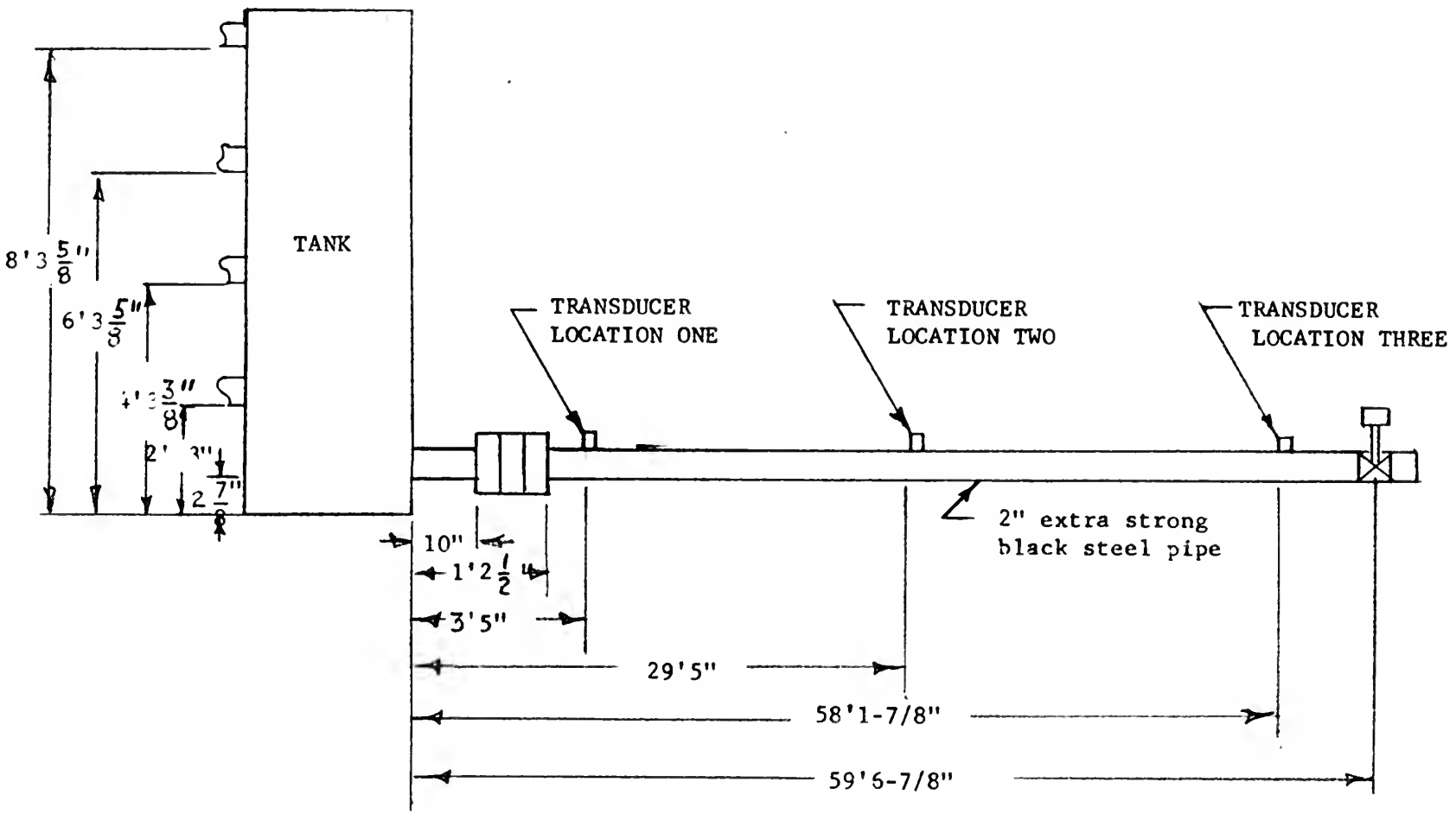


Fig. 13 Pipe and Tank Dimensions.

APPENDIX B

THEORY DERIVATIONS

1. The following is the derivation for equation (1) of the theory section as given by Stepanoff /13/. Newton's second law is as follows:

$$F = \frac{d(MV)}{dt_i} \qquad \text{(B-1)}$$

Where: F = Force, lbf.

V = Velocity, ft/sec.

$t_i$ = Time, sec.

M = Mass, slugs.

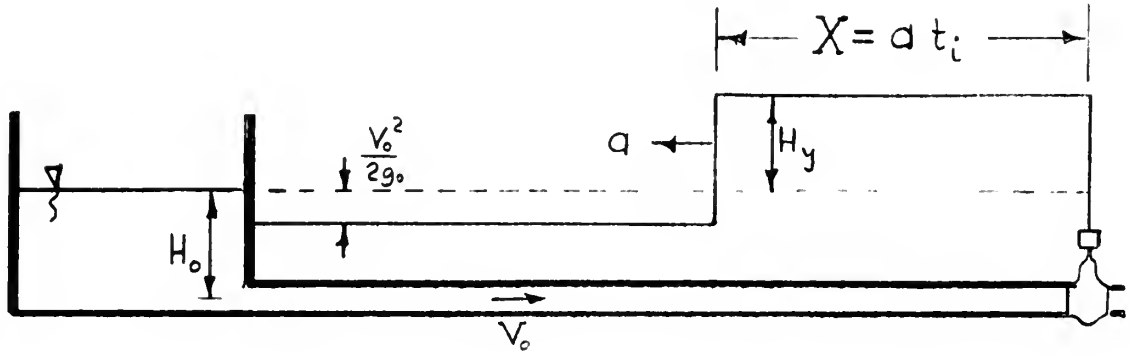


The velocity through the pipe ($V_o$) before valve closure is constant. The force (increase in pressure at the valve) is equal to the time rate change of momentum of the moving mass. The pressure-force relationship is as follows:

$$F = A \gamma H_y \qquad \text{(B-2)}$$

At time $t_i$ after closure the portion of the fluid in the length of pipe, X, will have its velocity reduced to zero, then:

$$F = A \gamma H_y = \frac{A\gamma}{g_o}\left(\frac{X}{t_i}\right) V_o \qquad \text{(B-3)}$$

Where: A = Pipe internal cross sectional area, $ft^2$

$\gamma$ = Specific weight of fluid flowing, $lbm/ft^3$.

$H_y$ = Head rise above initial no flow static head, $H_o$, ft of water

$g_o$ = Proportionality constant in Newton's second law of motion, (lbm-ft)/(lbf-sec$^2$)

X = Distance to any position on the pipe measured from the valve, ft.

$t_i$ = Time after closure, sec.

$V_o$ = Velocity of fluid in the pipe before valve closure, ft/sec.

The term $\frac{A\gamma X}{g_o t_i}$ in equation (B-3) is the mass flow rate. In equation (B-3), $X/t_i$ is the velocity of the pressure pulse, a. Substituting a and cancelling the $\gamma A$ term on both sides of the equation (B-3) gives:

$$H_y = a \frac{V_o}{g_o} \qquad (1)$$

2. The derivation of equation (2) in the theory section as given by Stepanoff /13/, is as follows. After instantaneous valve closure a region of compressed water is created adjacent to the valve and extends a distance X at time $t_i$ after closure. The pipe in this region expands under pressure from $D_o$ to $D_1$. From the instant of closure until $t_i$ a volume of water equal to $AV_o t_i$ passes through the original cross section at X. There is no outlet for the water; therefore, the volume must be accommodated by expanding the pipe radially and by compressing the water.

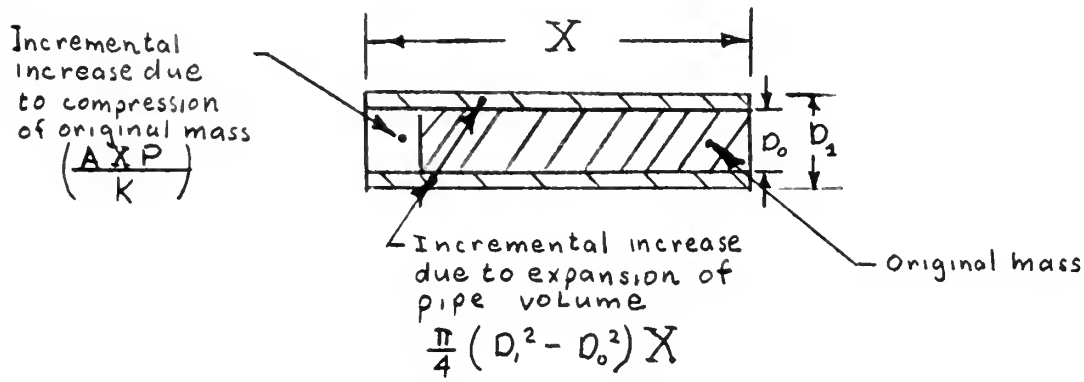

The increase in volume caused by the compression of the water in the pipe is obtained from the definition of bulk modulus as follows:

$$K_w = -G_w \frac{dP}{dG_w} = -G_w \frac{P}{\Delta G_w} \tag{B-4}$$

Where: $K_w$ = Water bulk modulus, $lbf/ft^2$.

$G_W$ = Volume, $ft^3$

$\Delta G_W$ = Incremental change in volume, $ft^3$

P = Incremental change in pressure caused by the velocity head changing to pressure head, $lbf/ft^2$.

Solving equation (B-4) for $\Delta G_W$ gives:

$$\Delta G_w = \frac{-G_w P}{K_w} \tag{B-5}$$

but the original volume $G_W$ is equal to AX. Substituting AX for $G_W$ gives:

$$\Delta G_w = \frac{-AXP}{K_w} \tag{B-6}$$

The negative sign indicates that $\Delta G$ decreases with increasing pressure. The decreased volume is used to accommodate the additional mass that enters the section of Pipe X feet long. The volume made available by the compression of the original water is:

$$\Delta G_w = \frac{AXP}{K_w} \tag{B-7}$$

The increased volume caused by the expanding of the pipe is:

$$\Delta G_p = \frac{\pi}{4}\left(D_i^2 - D_o^2\right)X \tag{B-8}$$

By equating the additional volume of water that must be accommodated ($AV_o t_i$) to the volume that the pipe expands plus the volume that the water compresses the following is obtained:

$$A V_o t_i = \frac{A X P}{K_w} + \frac{\pi}{4}(D_1^2 - D_o^2) X \qquad \text{(B-9)}$$

For the pipe

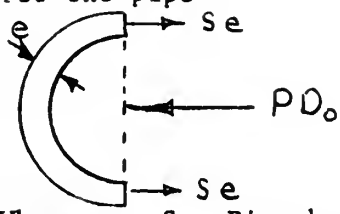


$$P D_o = 2 S e \qquad \text{(B-10)}$$

Where: S = Pipe hoop stress, $lbf/ft^2$.

e = Pipe wall thickness, ft.

Hooke's law for the pipe expansion is:

$$S = E\left(\frac{D_1 - D_o}{D_o}\right) \qquad \text{(B-11)}$$

Where: E = Modulus of elasticity, $lbf/ft^2$.

Combining equations (B-10) and (B-11) gives:

$$\frac{P D_o}{2 e E} = \frac{D_1 - D_o}{D_o} \qquad \text{(B-12)}$$

In equation (B-9) $D_1^2 - D_o^2$ may be written $(D_1+D_o)(D_1-D_o)$.

Since $D_1 - D_o$ is very small compared to $D_1$ or $D_o$, the term $(D_1+D_o)$ may be written $2D_o$. Then the last term of equation (B-9) becomes:

$$\frac{\pi X (D_1 + D_o)(D_1 - D_o)}{4} = \frac{X \pi D_o (D_1 - D_o)}{2} \qquad \text{(B-13)}$$

Multiplying both sides of equation (B-12) by $D_o$ gives:

$$D_1 - D_o = \frac{P D_o^2}{2 e E} \qquad \text{(B-14)}$$

Substituting equation (B-14) into equation (B-13) and substituting A for the cross sectional area term, $\frac{\pi D_o^2}{4}$ gives

$$\frac{X \pi (D_1^2 - D_o^2)}{4} = \frac{X A D_o P}{e E} \qquad \text{(B-15)}$$

Substituting equation (B-15) for the last term in equation (B-9) gives:

$$V_o A t_i = \frac{X P A}{K_w} + \frac{X D_o P A}{e E}$$

$$V_o t_i = X P \left( \frac{1}{K_w} + \frac{D_o}{e E} \right) \qquad \text{(B-16)}$$

The term $X/t_i$ is the wave velocity, a. Substituting and solving for a gives:

$$a = \frac{V_o}{\left( \frac{1}{K_w} + \frac{D_o}{e E} \right)} \qquad \text{(B-17)}$$

If equation (1) is multiplied by the specific weight of water ( $\gamma_w$), the following is obtained:

$$H_y \gamma_w = P = \frac{a V_o \gamma_w}{g_o} \qquad \text{(B-18)}$$

Solving (B-18) for $V_o$ gives:

$$V_o = \frac{P g_o}{a \gamma_w} \qquad \text{(B-19)}$$

Substituting (B-19) into (B-17) and letting D equal $D_o$ and $\rho_w$ equal $\frac{\gamma_w}{g_o}$ gives:

$$a = \frac{1}{\sqrt{\rho_w \left( \frac{1}{K_w} + \frac{D}{e E} \right)}} \qquad (2)$$

The maximum theoretical pressure rise, ($P_{NT}$) is given by substituting equation (2) into equation (B-18).

$$P_{NT} = \frac{V_o \gamma_w}{g_o \sqrt{\rho_w \left( \frac{1}{K_w} + \frac{D}{e E} \right)}} \qquad (4)$$

The experimental results were expressed as $P/P_{NT}$.

$$\frac{P}{P_{NT}} = \frac{P \sqrt{\rho_w \left( \frac{1}{K_w} + \frac{D}{e E} \right)}}{V_o \gamma_w} \qquad \text{(B-20)}$$

The term P is the experimental pressure rise above the no flow static pressure.

3. The following is the derivation of equations (3), (3a), (5), (5a), (6), and (6a) of the theory section. These derivations are based upon work done by Karplus /4/. His equations were modified to make them apply to the water hammer model. The following is a form of equations (2) for an air-water mixture.

$$a^{-2} = \rho_c \left[ \mathcal{K}_c + \frac{D}{eE} \right] \tag{B-21}$$

Where: Subscript c represents the air-water mixture.

$\mathcal{K}_c = \frac{1}{K_c}$ = Air-water mixture compressibility, $ft^2/lbf$.

The density of the mixture ($\rho_c$) is given by:

$$\rho_c = \frac{M_a + M_w}{G_c} = \frac{M_a}{G_c} + \frac{M_w}{G_c} \tag{B-22}$$

Where: G = Volume, $ft^3$.

M = Mass, slugs.

<u>subscripts</u>

a = Air

W = Water

Because mass is the product of density and volume, $\rho_c$ becomes:

$$\rho_c = \frac{G_a \rho_a}{G_c} + \frac{G_w \rho_w}{G_c} \tag{B-23}$$

The volume fraction of air is defined as:

$$x = \frac{G_a}{G_c} \tag{B-24}$$

The volume fraction water is defined as:

$$(1-x) = \frac{G_w}{G_c} \tag{B-25}$$

Substituting (B-24) and (B-25) into (B-23) gives:

$$\rho_c = x \rho_a + (1-x) \rho_w \tag{B-26}$$

Compressibility is defined as follows:

$$\mathcal{K}_c = -\frac{dG_c}{G_c dP} = \frac{-(dG_a + dG_w)}{G_c\, dP}$$

$$= -\frac{dG_w}{G_w dP}\left(\frac{G_w}{G_c}\right) - \frac{dG_a}{G_a dP}\left(\frac{G_a}{G_c}\right) \qquad \text{(B-27)}$$

Substituting equations (B-24) and (B-25) into (B-27) gives:

$$\mathcal{K}_c = (1-x)\,\mathcal{K}_w + x\,\mathcal{K}_a \qquad \text{(B-28)}$$

Substituting equations (B-26) and (B-28) into equation (B-21) gives:

$$a^{-2} = \left[(1-x)\rho_w + x\rho_a\right]\left[x\,\mathcal{K}_a + (1-x)\,\mathcal{K}_w + \frac{D}{eE}\right] \qquad \text{(B-29)}$$

Rearranging equation (B-29) gives:

$$a^{-2} = x^2\rho_a\mathcal{K}_a + (1-x)^2\rho_w\mathcal{K}_w + x(1-x)\left[\rho_a\mathcal{K}_w + \rho_w\mathcal{K}_a\right] + \frac{D}{eE}\left[(1-x)\rho_w + x\rho_a\right] \qquad \text{(B-30)}$$

For isothermal conditions and assuming the ideal gas law applies:

$$\mathcal{K}_{Ia} = \frac{1}{P_{ABS}} \qquad \text{(B-31)}$$

Where: $P_{ABS}$ = Absolute pressure of system, $lbf/ft^2$.

$\mathcal{K}_{Ia}$ = Isothermal compressibility of air, $ft^2/lbf$

The velocity of sound in air is given as:

$$a_a^{-2} = \mathcal{K}_{Aa}\rho_a \qquad \text{(B-32)}$$

Where $\mathcal{K}_{Aa}$= Adiabatic compressibility of air, $ft^2/lbf$.

For adiabatic conditions and assuming the ideal gas law applies:

$$\mathcal{K}_{Aa} = \frac{1}{k\,P_{ABS}} \qquad \text{(B-33)}$$

Where: k = ratio of specific heat of air at constant pressure to that at constant volume, 1.403 for air

By combining equations (B-31) and (B-33), the following is obtained:

$$\mathcal{K}_{Ia} = k\,\mathcal{K}_{Aa} \tag{B-34}$$

The velocity of sound in water is given by:

$$a_w^{-2} = \rho_w \mathcal{K}_w \tag{B-35}$$

For isothermal conditions substitute (B-32), (B-33), (B-34), and (B-35) into (B-30). This gives:

$$a_I^{-2} = \frac{x^2 k}{a_a^2} + \frac{(1-x)^2}{a_w^2} + x(x-1)\left[\frac{\rho_w}{P_{ABS}} + \rho_a \mathcal{K}_w\right] + \frac{D}{eE}\left[(1-x)\rho_w + x\rho_a\right] \tag{3}$$

Using the adiabatic conditions for equations (B-30) gives the following results:

$$a_A^{-2} = \frac{x^2}{a_a^2} + \frac{(1-x)^2}{a_w^2} + x(1-x)\left[\frac{\rho_w}{k P_{ABS}} + \rho_a \mathcal{K}_w\right] + \frac{D}{eE}\left[(1-x)\rho_w + x\rho_a\right] \tag{3a}$$

For isothermal conditions for an air-water mixture equation (B-18) becomes:

$$P = \frac{V_o \gamma_c a_I}{g_o} \tag{B-36}$$

Where: $a_I$ is given by equation (3).

Substituting equation (B-36) into (B-20) gives:

$$\left(\frac{P}{P_{NT}}\right)_T = \frac{\gamma_c a_I}{\gamma_w} \sqrt{\rho_w \left(\frac{1}{K_w} + \frac{D}{eE}\right)} \tag{6}$$

Where: $a_I$ is given by equation (3).

For adiabatic conditions:

$$\left(\frac{P}{P_{NT}}\right) = \frac{\gamma_c a_A}{\gamma_w}\sqrt{\rho_w\left(\frac{1}{K_w} + \frac{D}{eE}\right)} \qquad (6a)$$

Where: $a_A$ is given by equation (3a).

## APPENDIX C

## EQUIPMENT

1. The head tank consisted of a tank which was two feet in diameter at the lower end and one foot ten and one-half inches at the upper end. The upper part of the tank was light sheet metal and the lower part of the tank was plate steel. Two inch overflow lines were provided at approximately two foot intervals as is shown in Appendix A. These overflow lines were standard two inch galvanized steel pipe. Each overboard line had a two inch gate valve in the line. All the overboard lines ran into a common line which discharged into a collecting tank open to the atmosphere. This collecting tank had a drain which discharged into the main sewage system. A Weston thermometer located near the bottom of the tank, was used to measure the inlet water temperature.

The main run of pipe consisted of two inch extra strong black steel pipe. The outside diameter was 2.375 inches, the inside diameter was 1.939 inches. The wall thickness was 0.218 inches. Three sections of pipe were welded together. Care was taken to insure good butting of the individual sections. At the transducer locations, transducer fittings one inch in diameter and one inch high were welded into the pipe. These fittings had standard 14 mm by 1.25 automotive spark plug threads.

The water weigh system consisted of a Toledo Scales Company platform scales with a capacity of 1600 pounds and a steel plate rectangular tank, 20 inches by 28 inches by 20 inches. A 3 inch by 3 inch section was cut out of the top to permit entrance of the discharge pipe. This tank had two, 2 inch gate valves for discharge. They discharged into drain lines to the sewage system.

The following scale information is provided.

| | |
|---|---|
| Manufacturer | Toledo Scales Company<br>Toledo, Ohio |
| Model | 31-1811FC |
| Serial Number | 2180-0-225 |
| Capacity | 0-1600 pounds |

An electric timer, which measured to the nearest one tenth of a second, was used to measure the time to fill the weigh tank with water.

2. The air injection system is shown schematically as part of Fig. 1. A photograph of the air injection system is shown in Fig. 2. The source of air was from the 125 psi air system permanently installed in Building 500, at the United States Naval Postgraduate School. This system was reduced to approximately fifteen psi by a regulating valve. One-quarter inch vinyl tubing was used from the regulating valve to a pipe manifold. A copper-constantan thermocouple was installed in the pipe manifold to measure the temperature of the air. A Rubicon Company catalog number 2732 potentiometer was used to measure the thermocouple output. This is item 1 in Fig. 2. To measure the pressure of the air a 50 inch mercury manometer was used. A one-quarter inch vinyl tubing line was tapped into the air manifold. This line was connected to the mercury manometer. The other side of the manometer was open to the atmosphere. Item 4 of Fig. 2 shows this manometer. From the manifold a one-quarter inch vinyl line led to the rotometer. The following data is provided.

| | |
|---|---|
| Manufacturer | Fisher-Porter Company |
| Flowrotor tube number | 2-F-1/4-20-5/70 |
| Float | glass |
| Range (14.7 psi, 70°F) | 0-0.325 $ft^3$/min. |

The manufacturer's calibration curve, converted from cubic centimeters per minute to cubic feet per minute, was used. Fig. 14 is a copy of this curve. Four points on this curve were checked using American Meter Company wet gas meter A1-20-11472.

The flow rate was corrected to 14.7 psia and 70°R for each run using the following relationship suggested by the manufacturer /2/.

$$Q_a = Q_u \sqrt{\left(\frac{P_a}{14.7}\right)\left(\frac{530}{T_a}\right)} \qquad \text{C-1}$$

$Q_a$ = $ft^3$/min at 70°F, 14.7 psia

$P_a$ = pressure at which measurement was made, psia

$T_a$ = temperature at which measurement was made, °R.

$Q_u$ = flow rate in $ft^3$/min taken from the curve of Fig. 14. This curve was entered with the rotometer reading.

Item number 2 in Fig. 2 shows the rotometer. A one-quarter inch vinyl tubing connected the rotometer with a manual control valve. The control valve was used to control the air flow rate. From the control valve a one-quarter inch vinyl tube led to a manifold section in the pipe. A stop valve was provided for each of these separate lines. Item 5 of Fig. 2 shows the equipment used for the injection of the air into the pipe. Three separate rings of holes were used to inject the air. One ring consisted of two holes, each with a diameter of 0.04 inches. The second ring consisted of four holes, each with a diameter of 0.07 inches. The third ring consisted of eight holes with diameters of 0.07 inches. These holes were equally spaced around the circumference of the pipe. A plexiglass ring, four inches in diameter, with a circumferential groove for air injection was provided for each ring of holes. These rings were sealed with "O" rings. Fig. 5 shows a cross sectional view of this system. The system was

designed so that any one of the rings could be used. However, it was not necessary to do this. All experimental work was done with air entering all three rings of holes.

3. The valve and closure system is shown in Fig. 3. The quick closing valve was a modified standard Crane two inch quick closing gate valve. The valve was modified by screwing on a steel disc two inches in diameter and one inch high on the top of the stem. This disc was the point of impact for the falling weight which closed the valve. A mechanism was designed to hold the valve closed when it was in the shut position. A stand that was completely isolated from the piping system was used to stop the valve. By using this method, the full impact of the stopping valve was not transmitted to the piping system. A seven pound cylindrical steel bar one inch in diameter by 24 inchs long was used as the weight for closing the valve. This weight was dropped through an aluminum pipe, one and one-quarter inches in diameter. This aluminum pipe contained numerous air holes to allow the weight to fall freely. Appendix G contains preliminary calculations used to estimate the closure time. The weight was dropped from nine feet for all runs. The closure time of the valve was measured with an oscilloscope. The time sweep of the oscilloscope was triggered by a photoelectric cell. A contact completed a 45 volt direct current circuit when the valve was closed. This voltage was put across the vertical plates of the oscilloscope. A Polaroid time exposure was made of the oscilloscope, the closure time was taken from the photograph. Polaroid 3000 speed film was used.

The quick release mechanism consisted of a steel pin which held the weight nine feet above the valve. A line was attached to this pin. When it was desired to drop the weight, the pin was pulled and the weight fell.

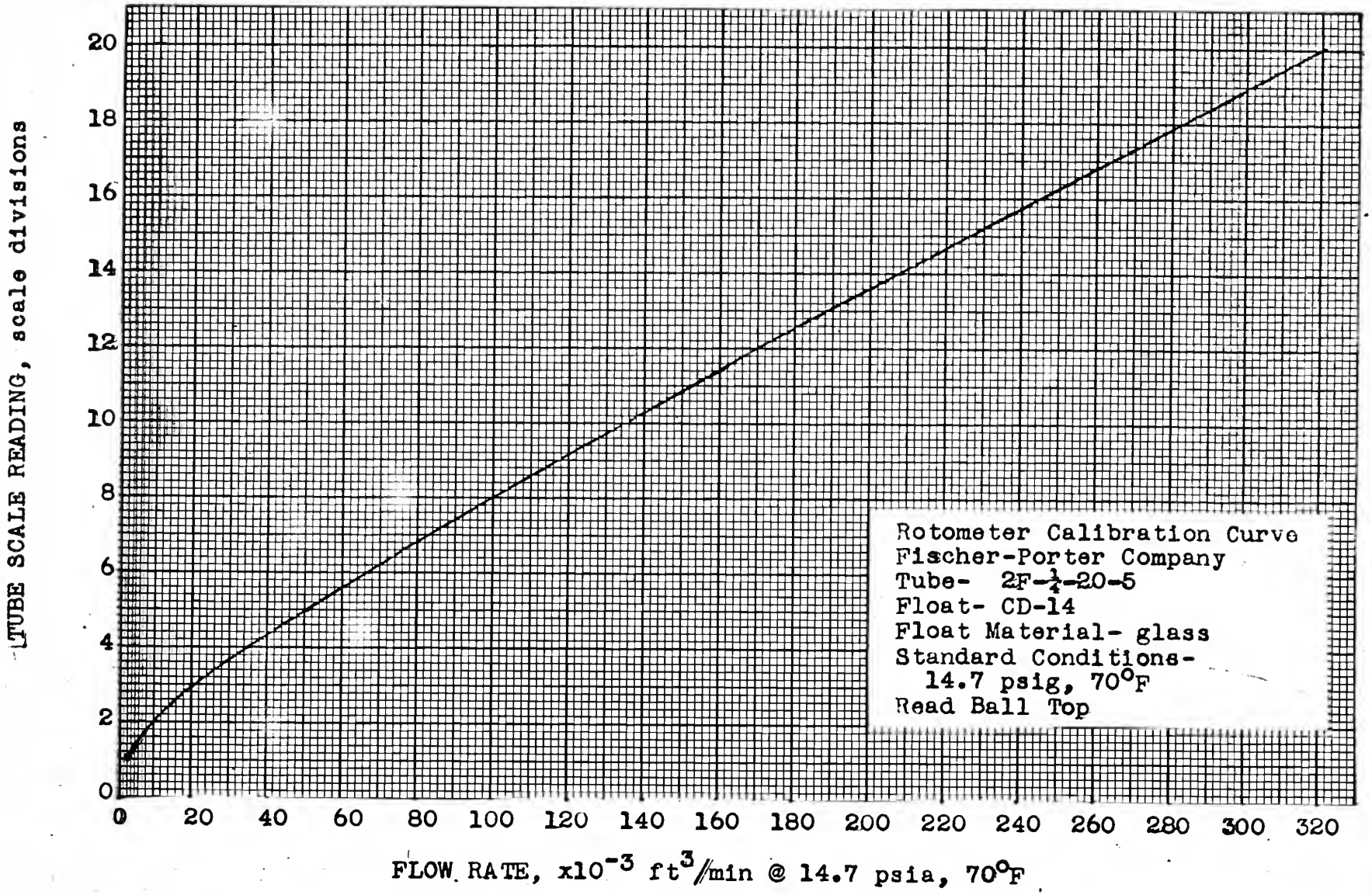


FIG. 14. Rotometer Calibration Curve

A nylon string was attached to the weight. This was used with a pulley to pull the weight to the desired height above the valve.

4. Selected characteristics of the pressure sensing equipment are given below. For complete details refer to manufacturer's instruction book /5/.

Kistler 401 Pressure Transducer

| | |
|---|---|
| pressure range | 0.0-3000 psi |
| overload capacity | 50% |
| linearity | 1% |
| natural frequency | 48,000 cps |
| maximum continuous temperature | 500°F |
| maximum intermittent temperature | 3000°F |
| length | 2.04 in. |
| diameter | 0.625 in. |
| weight | 1.75 oz. |
| serial number | #1044 |

Kistler Model 651 Piezo Calibrator

| | |
|---|---|
| input voltage, maximum | 0.6 volts |
| output voltage, maximum | 0.3 volts |
| voltage gain | 0.5 |
| input impedance | $10^{14}$ ohms |
| output impedance | $10^{5}$ ohms |
| frequency range | 0-10 kc |
| linearity | 1% |
| dimensions | 7 x 10 x 6 in. |
| weight | 4.7 lbm |

Hewlett Packard Model 130 Oscilloscope

| | |
|---|---|
| internal sweep accuracy | 5% |

Vertical and Horizontal Amplifiers

| | |
|---|---|
| frequency response | 0-300 kc |
| sensitivity | 1mv/cm-20 volts/cm |
| accuracy | 5% |
| input impedance | 1 megohm |

Cathode Ray Tube

| | |
|---|---|
| power requirements | 115/230 volts, AC<br>50/400 cps, approximately<br>175 watts |
| dimensions | 9 3/4 in. by 15 in. by 21-1/4 in. |
| weight | 39 lbm |

Kistler transducer model 401 serial number 1044 was calibrated using an Ashcroft dead-weight tester. The system used for calibration was the same as shown in Fig. 4 except the transducer was inserted into the 14 mm dead-weight adapter fitting instead of the pipe. Sweeney /14/ describes the procedure for using the dead-weight tester. The important thing in calibrating was to rotate the weights when loading the transducer. The transducer was rapidly loaded so that there would be no error due to charge leakage from the crystal. The transducer was calibrated for the calibrator range scales of 10 and 100. The 10 range covers 0-125 psig and 100 range covers 0-1250 psig. Fig. 15 and 16 show these calibration curves. These curves show the readings on the calibrator for a given pressure. It was necessary to determine the number of calibration divisions that correspond to a centimeter deflection on the oscilloscope. Knowing this and using the calibration curves, the psig/centimeter on the oscilloscope was calculated. For the oscilloscope used for this experimental

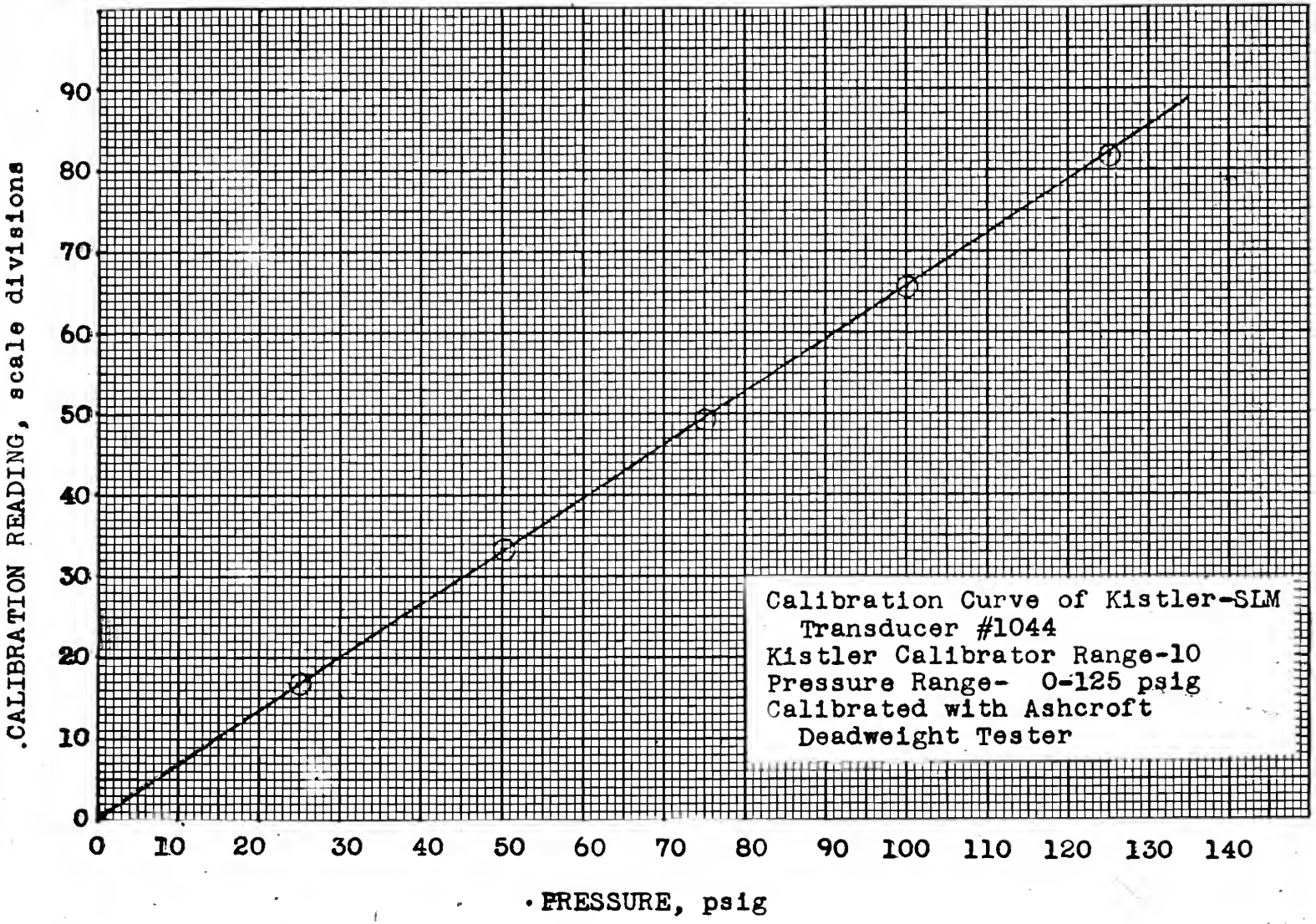


FIG. 15. Transducer Calibration Curve, 0 - 125 psig

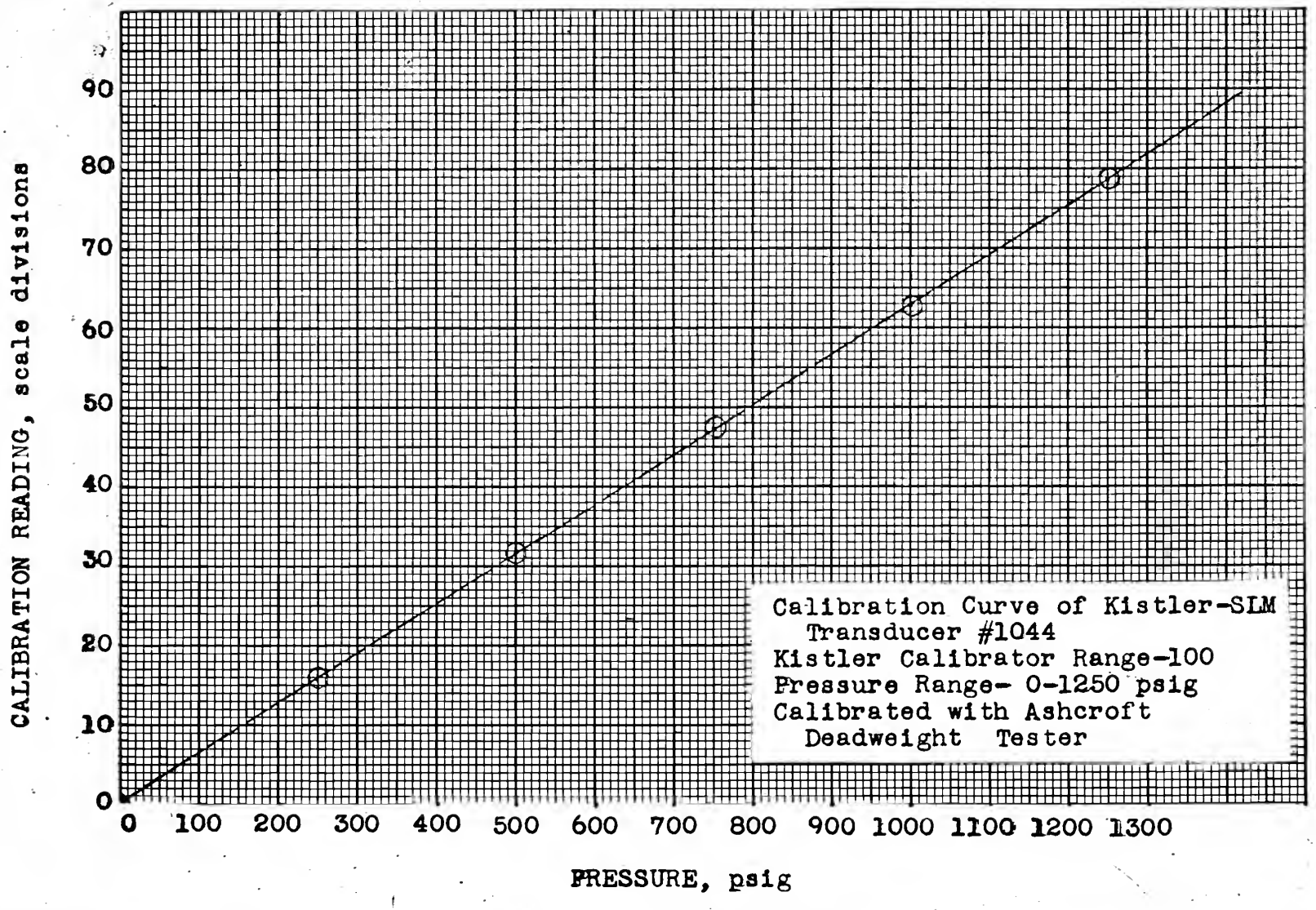


FIG. 16. Transducer Calibration Curve, 0-1250 psig

work, the following values were obtained and used. These values are for Kistler model 401 serial number 1044 pressure transducer.

| Calibrated range | Oscilloscope scale | Calibration divisions/ 10 cm oscilloscope deflection | psig/cm |
|---|---|---|---|
| 10 | 5 mv/cm | 19.7 | 3.0 |
| 10 | 10 mv/cm | 39.1 | 6.0 |
| 10 | 20 mv/cm | 77.2 | 11.8 |
| 100 | 5 mv/cm | 17.2 | 26.6 |
| 100 | 10 mv/cm | 34.4 | 54.4 |
| 100 | 20 mv/cm | 67.8 | 106.9 |

## APPENDIX D

## DETAILED PROCEDURE FOR A RUN

The detailed step by step procedure for each run was as follows:

1. Record atmospheric temperature and pressure.
2. Fill the tank to the level desired.
3. Open quick closing stop valve.
4. Adjust water inlet to the tank until the overflow at the desired level is just a trickle.
5. Adjust the air rotometer to desired flow rate with the control valve immediately following the rotometer in the air inlet system.
6. Insure weigh tank discharge valves are completely open and that the tank is as low as possible.
7. Set electric timer to zero.
8. Close weigh tank discharge valves.
9. Start timer and record initial weight on scales when the timer is started.
10. Fill weigh tank until it is nearly full.
11. Record weight and time at nearly full position.
12. Open weigh tank discharge valves.
13. Lift weight to nine foot position and insert quick release pin.
14. Record inlet and outlet water temperatures.
15. Record rotometer setting (read ball top).
16. Record air mercury manometer readings.
17. Record air temperature.

18. Set calibrator range to desired position. Insure the meter is adjusted to 1.0. Allow a ten minute warm up period for the calibrator and the oscilloscope.
19. Set oscilloscope on desired vertical scale.
20. Adjust oscilloscope sweep rate to the desired time scale.
21. Insure the SYNC switch is set to external trigger (EXT) on the oscilloscope.
22. Insure that battery is properly connected to trigger circuit of the oscilloscope.
23. Set the horizontal sensitivity of the oscilloscope to internal sweep.
24. Check system by checking the calibration reading for ten centimeters deflection on the vertical scale of the oscilloscope.
25. Adjust vertical and horizontal position until the oscilloscope trace is in desired position.
26. Set camera on time exposure.
27. Open camera shutter.
28. Close valve by dropping the weight with the quick release mechanism.
29. Close camera shutter.
30. Open quick closing valve.
31. Develop Polaroid photograph.

| APPENDIX E SAMPLE DATA SHEET | | | | | | | | | | | | | | | | |
|---|---|---|---|---|---|---|---|---|---|---|---|---|---|---|---|---|
| RUN # 3-9- | | | 1 | 2 | 3 | 4 | 5 | 6 | 7 | 8 | 9 | 10 | 11 | | | |
| $P_{ATM}$ | | in Hg | 30.264 | | | | | | | | | | | | | |
| $t_{ATM}$ | | °F | 76 | | | | | | | | | | | | | |
| AIR | | | | | | | | | | | | | | | | |
| $t_a$ | | °F | [illegible] | 70.6 | 70.6 | 70.6 | 70.6 | 70.4 | 70.6 | 70.6 | 70.6 | 70.6 | 70.6 | | | |
| $P_a$ | $P_{1a}$ | in Hg | - | 14.50 | 14.10 | 13.51 | 13.48 | 14.41 | 13.99 | 13.18 | 13.10 | 12.62 | 12.56 | | | |
| | $P_{2a}$ | in Hg | - | 14.40 | 14.01 | 13.43 | 13.39 | 14.32 | 13.90 | 13.02 | 13.02 | 12.55 | 12.49 | | | |
| ROTOMETER, | SCALE DIV. | | 0 | 4.2 | 4.2 | 8.2 | 8.2 | 12.2 | 12.2 | 16.2 | 16.2 | 20.2 | 20.2 | | | |
| WATER | | | | | | | | | | | | | | | | |
| NOMINAL HEAD, | | ft | 8 | 8 | 8 | 8 | 8 | 8 | 8 | 8 | 8 | 8 | 8 | | | |
| [SCALE WEIGHT] | 1 | lbm | 130 | 120 | 120 | 120 | 120 | 130 | 130 | 130 | 130 | 110 | 110 | | | |
| | 2 | lbm | 298 | 290 | 290 | 290 | 290 | 300 | 300 | 300 | 300 | 300 | 300 | | | |
| WEIGH TIME | | sec | 17.5 | 18.1 | 18.1 | 18.4 | 18.4 | 18.7 | 18.7 | 18.8 | 18.8 | 21.4 | 21.4 | | | |
| TEMP. | IN | °F | 56 | 56 | 56 | 56 | 56 | 56 | 56 | 55 | 56 | 56 | 56 | | | |
| | OUT | °F | 56 | 56 | 56 | 56 | 56 | 56 | 56 | 55 | 56 | 56 | 56 | | | |
| MISC. | | | | | | | | | | | | | | | | |
| TRANSDUCER LOCATION | | | 2 | 2 | 2 | 2 | 2 | 2 | 2 | 2 | 2 | 2 | 2 | | | |
| HEIGHT WEIGHT DROPPED | | ft | 9 | 9 | 9 | 9 | 9 | 9 | 9 | 9 | 9 | 9 | 9 | | | |
| OSCILLOSCOPE DATA | | | | | | | | | | | | | | | | |
| CALIBRATOR RANGE | | | 100 | 10 | 10 | 10 | 10 | 10 | 10 | 10 | 10 | 10 | 10 | | | |
| CAL DIV/10 cm DEFLECTION | | | 34.4 | 39.1 | 39.1 | 39.1 | 39.1 | 39.1 | 39.1 | 39.1 | 39.1 | 39.1 | 39.1 | | | |
| TIME SCALE | | sec/cm | 0.01 | 0.1 | 0.1 | 0.1 | 0.1 | 0.1 | 0.1 | 0.1 | 0.1 | 0.1 | 0.1 | | | |
| VERTICAL SCALE | | mv/cm | 10 | 10 | 10 | 10 | 10 | 10 | 10 | 10 | 10 | 10 | 10 | | | |

## APPENDIX F

## SAMPLE CALCULATIONS

Sample calculations have been included for run number 3-9-10. The data for this run has been included on the sample data sheet in Appendix E.

$P_{ATM}$ = 30.264 in. Hg

$t_{ATM}$ = 76.0°F

c = -0.129 Barometer temperature correction

Calculate atmospheric pressure in psia

$$(P_{ATM}(\text{in Hg}) + c)(0.4913) = P_{ATM}(\text{psia})$$

$$(30.264-0.129)(0.4913) = 14.81 \text{ psia}$$

where 0.4913 is the conversion factor for converting pressure in inches of Hg to psia.

Calculate absolute pressure of air.

$$(P_{1a} + P_{2a})\ (0.4913) + P_{ATM} = P_a(\text{psia})$$

$P_{1a}$ and $P_{2a}$ are the inches of mercury measured on each leg of the air manometer.

$P_{1a}$ = 12.62 in. Hg

$P_{2a}$ = 12.55 in. Hg

$P_{ATM}$ = 14.81 psia

$P_a$ = pressure at which air was measured, psia

$$(12.62 + 12.55)(0.4913) + 14.81 = 27.18 \text{ psia}$$

Calculate air flow rate at 14.7 psia and 70°F.

$$Q_a = Q_u \sqrt{\left(\frac{P_a}{14.7}\right)\left(\frac{530}{T_a}\right)}$$

where:

$Q_a$ = air flow rate at 14.7 psia and 70°F, $ft^3/min$.

$Q_u$ = uncorrected air flow rate taken from Fig. 14.

Enter Fig. 14 with rotometer setting.

$T_a$ = Absolute temperature at which air flow rate was measured, °R

$$Q_a = 0.325 \sqrt{\left(\frac{27.18}{14.7}\right)\left(\frac{530}{530.6}\right)} = 0.442 \text{ ft}^3/\text{min}$$

Calculate mass flow rate of air

$$\dot{m}_a = Q_a \gamma_a$$

where:

$\dot{m}_a$ = Mass flow rate of air, lbm/min

$\gamma_a$ = Specific gravity of air at 14.7 psia and 70°F.

$\dot{m}_a = (0.442)(0.0752) = 0.03403$ lbm/min

Calculate volume flow rate at inlet water conditions

$$Q_{aw} = Q_a\left(\frac{14.7}{P_w}\right)\left(\frac{T_w}{530}\right)$$

where:

$Q_{aw}$ = Air volume flow rate at conditions of water inlet

$P_w$ = Absolute pressure of water at air inlet, psia

$T_w$ = Absolute temperature of air at water inlet, °R

$$Q_{aw} = 0.442\left(\frac{14.7}{18.265}\right)\left(\frac{516}{530}\right) = 0.3463 \text{ ft}^3/\text{min}$$

Calculate the water mass flow rate

$$\dot{m}_w = \frac{m_w(60)}{t_i}$$

$\dot{m}_w$ = Water mass flow rate, lbm/min

$m_w$ = Weight of water weighed in time $t_i$, lbm

$t_i$ = time to measure $m_w$ pounds of water, sec

$$\dot{m}_W = \frac{(190)(60)}{21.4} = 534 \text{ lbm/min}$$

Calculate water volume flow rate

$$Q_W = \frac{\dot{m}_w}{\gamma_w}$$

where:

$Q_W$ = Water volume flow rate, $ft^3/min$

$\gamma_W$ = Specific weight of water, $lbm/ft^3$

$$Q_W = \frac{534}{62.4} = 8.56 \text{ ft}^3/\text{min}$$

Calculate the volume percent air in mixture

$$\eta = \frac{Q_{aW}(100)}{Q_{aW}+Q_W}$$

where:

$\eta$ = Volume percent air at water inlet conditions %

$$\eta = \frac{(0.3463)(100)}{(0.3463 + 5.56)} = 3.89\%$$

Calculate the weight percent air in the mixture

$$\eta_{WT} = \frac{\dot{m}_a(100)}{\dot{m}_a + \dot{m}_w}$$

where:

$\eta_{WT}$ = Weight percent air in air water mixture, %

$$\eta_{WT} = \frac{(0.03403)(100)}{(0.03403 + 534)} = 0.00637\%$$

Calculate the maximum pressure

P = d•C-J

P = Pressure above the static no flow pressure, psi

C = Psi/cm of oscilloscope deflection, psi/cm

d = Deflection of oscilloscope, cm

J = Correction for velocity head at the location when the oscilloscope scale was zeroed, psi.

To determine the J correction, the difference in static pressure with flow and with no flow was experimentally measured for each head at each location. It was necessary to make this correction because the oscilloscope was zeroed for each run when there was velocity head in the pipe.

$$P = (3.1)(6.0)-2.1 = 16.5 \text{ psi}$$

Calculate pressure ratio $P/P_{NT}$

$$P/P_{NT} = \frac{P}{H_y \gamma_w} = \frac{P}{\left(\frac{V_o \gamma_w}{g_o}\right)\left(\frac{1}{\sqrt{\rho_w\left(\frac{1}{K_w}+\frac{D}{eE}\right)}}\right)}$$

$$P/P_{NT} = \frac{P g_o \sqrt{\rho_w\left(\frac{1}{K_w}+\frac{D}{eE}\right)}}{V_o \gamma_w}$$

where:

$V_o$ = Velocity of the water through the pipe with no air, determined experimentally, ft/sec

$\rho_w$ = Density of the water, slugs/ft$^3$

$K_w$ = Bulk modulus of water, lb/ft$^2$

D = Inside diameter of pipe, in.

e = Pipe wall thickness, in.

E = Modulus of elasticity of pipe lbf/ft$^2$

$H_y$ = Theoretical maximum head rise above the initial static head, equation 1, ft of water

$$P/P_{NT} = \frac{(16.5)(32.2)\sqrt{\frac{1}{(310{,}000)(144)}+\frac{1.939}{(0.218)(29.4\times10^6)(144)}}}{(7.52)(62.4)}$$

$$P/P_{NT} = 0.0445$$

## APPENDIX G

## VALVE CLOSURE

The water hammer model of Fig. 1 was used to generate the pressure pulses. For the maximum pressure to be theoretically possible, the model required a valve which would close in less than $\frac{2(L-X)}{a}$ seconds.

where: L = The length of the pipe from the tank to the valve, ft.

X = The distance from a given location to the valve, ft.

a = The velocity of the pressure pulse in the pipe, ft/sec.

The speed of the pressure pulse in pure water in a two inch extra strong steel pipe is 4580 ft/sec. For the maximum pressure as given by equation (1) to be possible at transducer location two, the valve had to close to less than 0.0128 seconds. If there was 0.05 percent by volume air at the water inlet conditions the closure time required at transducer location two for the maximum pressure to be possible was 0.0351 seconds. With ten percent by volume air, the closure time required at transducer location two was 0.438 seconds or less. Since the pressure wave travels fastest in water with no air, this was the limiting condition. Therefore, to use transducer location two, a closure time of less than 0.0128 seconds was required.

A free falling seven pound weight starting with zero initial velocity and falling nine feet would have a velocity calculated as follows:

$$V = \sqrt{2gs}$$

$$V = \sqrt{2(32.2)(2)} = 24.0 \text{ ft/sec}$$

where g = acceleration of gravity, $ft/sec^2$

s = distance the weight falls, ft

V = velocity of the falling weight, ft/sec

With a 24.0 ft/sec. velocity, the time of closure would be:

$$t_i = \frac{S_v}{V}$$

where $t_i$ = time for valve gate to travel $S_v$ distance, sec

$S_v$ = distance valve gate travels for closure, ft

V = velocity of valve gate

$t_i = (1/6)(1/24) = 0.0069$ sec.

Assuming an plastic collision, the following calculations are made.

$$M_1V_1 = (M_2 + M_1)V_2$$

$$V_2 = \frac{M_1}{M_1+M_2} V_1$$

Assuming $M_2 = 1.75$ lbm $= 1.75/32.2$ slugs

$M_1 = 7$ lbm $= 7/32.2$ Slugs

$$V_2 = \left(\frac{7}{(7+1.75)}\right)(24) = 19.2 \text{ ft/sec.}$$

The closure time for the valve would be:

$$t_i = S_i/V_2 = \frac{1}{(6)(19.2)} = 0.0087 \text{ sec.}$$

The packing on the valve was loose enough that the valve closed freely with very little resistance. The weight of the valve stem and gate was 1.75 lbm.

Experimentally the closure time was measured as 0.007 seconds with an uncertainty of 0.003 seconds. The method of measuring the closure time has been discussed in Appendix C.

## APPENDIX H

## UNCERTAINTY ANALYSIS

The uncertainty for runs 3-9-2 and 3-9-10 are included here as representative examples of the uncertainty of the experimental work. Since the magnitude of the variables differs between runs, these values are to be considered only as representative. The method of analysis is that proposed by Kline and McClintock /6/ for single sample data.

| Run Number | 3-9-2 | % | 3-9-10 | % |
|---|---|---|---|---|
| Item, Units | Value ± Uncertainty | | Value ± Uncertainty | |
| $m_w$, lb/min | 563.6 ± 13.6 | 2.4 | 534 ± 12 | 2.2 |
| $Q_w$, $ft^3$/min | 9.03 ± 0.22 | 2.4 | 8.56 ± 0.19 | 2.2 |
| $m_w$, lb water | 170 ± 4 | 2.4 | 190 ± 4 | 2.1 |
| $t_i$, sec | 18.1 ± 0.1 | 0.6 | 21.4 ± 0.1 | 0.5 |
| $T_w$, °R | 516 ± 1 | 0.2 | 518 ± 1 | 0.2 |
| $P_w$, psia | 18.26 ± 0.07 | 0.4 | 18.26 ± 0.07 | 0.4 |
| $Q_u$, $ft^3$/min | 0.040 ± 0.004 | 1.0 | 0.325 ± 0.004 | 0.1 |
| $Q_a$, $ft^3$/min | 0.0562 ± 0.006 | 10.0 | 0.442 ± 0.0057 | 1.3 |
| $Q_{aw}$, $ft^3$/min | 0.04403 ± 0.00439 | 9.9 | 0.3463 ± 0.0047 | 1.4 |
| P, psia | 51.9 ± 6 | 10.6 | 17.1 ± 3 | 17.5 |
| $P/P_{NT}$, | 0.1121 ± 0.0129 | 10.6 | 0.0368 ± 0.0064 | 17.5 |
| $P_{atm}$, in. Hg | 30.264 ± 0.002 | 0.007 | 30.264 ± 0.002 | 0.007 |
| $T_{atm}$, °F | 76.0 ± 0.5 | 0.65 | 76.0 ± 0.5 | 0.65 |
| $\eta$, % | 0.485 ± 0.050 | 10.2 | 3.89 ± 0.77 | 0.8 |